Hindawi
Journal of Advanced Transportation
Volume 2022, Article ID 1550015, 22 pages
https://doi.org/10.1155/2022/1550015

Research Article

Connected Transit Bus Dynamic Priority Weight Modeling and Conflicting Request Resolution Control at the Signalized Intersection

Shuxian He,[1] **Haihang Han**,[2] **Huan Zhang**,[1] **Shanzhi Sun**,[2] **and Tony Z. Qiu**[1,3]

[1]*Intelligent Transportation System Research Center, Wuhan University of Technology, Wuhan, Hubei, China*
[2]*Zhejiang Scientific Research Institute of Transport, Hangzhou, Zhejiang, China*
[3]*Department of Civil and Environmental Engineering, University of Alberta, Edmonton, Alberta, Canada*

Correspondence should be addressed to Tony Z. Qiu; zhijunqiu@ualberta.ca

Received 28 April 2022; Revised 13 September 2022; Accepted 8 October 2022; Published 6 December 2022

Academic Editor: Jing Zhao

Multiaccess edge computing (MEC) and connected vehicle (CV) technologies have shown great potential and strength for traffic perception and real-time computing, which can be applied to enhance the efficiency of connected transit bus operations under their lower penetration conditions. Moreover, for the transit signal priority system, how to establish a model to measure traffic demand for conflicting priority request resolution and improve system response time has been widely researched for the last few decades. This paper proposes a dynamic priority weight (DPW) model for connected transit buses and a traffic signal control approach to coordinate multidirectional conflicting priority requests at a signalized intersection. The proposed model takes advantage of vehicle location, speed, and signal timing data to build time to change (TTOC) correlation functions to measure priority weights of both single-vehicle and directionality accumulation with consideration of vehicles arriving during the current green phase and conflict phase conditions; then, the aggregated priority weight value of each movement can be calculated in real-time. Once the maximum aggregated priority weight value among all movements is determined, the corresponding phase switch strategy is presented for the conflicting request resolution control problem. Homologous algorithm software for distributed deployment can be subsequently used for swift response. Simulation results show that the proposed DPW model-based traffic signal control method shows significant performance advancement, where the queueing vehicle number decrease exceeds 1 pcu/s and the throughput rate of major movements increases by approximately 2% without sacrificing the performance of minor movements in a large amount. What is more, it shows better delay optimization for social vehicles than the algorithm with delay as the objective while declining bus delay appreciable quantity with 43.4 s in average. Field test results also show that this method has excellent abilities to improve intersectional traffic capacity, for which queueing vehicle number and throughput rate indicators of all phases dramatically improved with 1.92 pcu/s and 6.68% on average, except for a slight degradation of individual minor traffic movements with 0.99 pcu/s and 0.11%.

1. Introduction

Public transportation has been widely accepted as one of the most effective strategies to alleviate traffic congestion. As a traffic demand-based closed-loop signal control system, compared with other transit bus services, e.g., urban bus lines, bus specific phases, transit signal priority (TSP) not only has fewer negative impacts on urban traffic operation but also sufficient competition for economic and public mobility, that can be applied to make transit buses more reliable, convenient, and comfortable [1]. Previous studies showed that proper enforcement of TSP could improve transit service levels without sacrificing the traffic efficiency of conflicting traffic movements, especially when advanced hardware and a highly flexible algorithm are provided. Accurate traffic detection systems, reasonable phase switch

strategies and swift request response mechanisms are three key components that have significant impacts on TSP performance [2, 3].

The existing TSP algorithm can be divided into three categories, passive TSP, active TSP, and real-time TSP [4–6]. Passive TSP changes signal timing permanently, even if transit buses are not present, and thus has negative impacts on vehicles in the nontransit approaches. However, that vehicle arrival pattern inferred from historical data rather than a detection device increases the necessity of steady traffic volume and stay duration at the bus station [6].

Active TSP has experienced progress from the unconditional to the conditional stage. Unconditional TSP algorithms address critical shortcomings by adopting detection technologies to selectively detect transit buses approaching the intersection; they are certainly given priority for delay reduction without any condition. Only with consideration of traffic conditions could signal control decisions be made with the conditional stage; the objective has evolved from decreasing bus delay to enhancing the reliability of bus services and the traffic efficiency of the intersection. Due to shortages of detection range, conventional detection devices are sometimes not appropriate under high-volume and long-queue traffic conditions [5].

Real-time TSP requires temporal and dimensional perception of vehicle location [7]. One type is infrastructure-based vehicle real-time motion state indirectly sensed by loop detectors, video detectors, or radar. Another type is vehicular, onboard equipment-based trajectory capture [8]. Advanced communication and swift computing systems, typically connected vehicles, and multiaccess edge computing technology are attracting the attention of many researchers and have been greatly developed and gradually applied in practice. Through vehicle-to-infrastructure communication, accurate transit bus speed, position, and priority request phase data can be obtained immediately, and the statistical inaccuracy of vehicular arrival and traditional detection device shortage issues can be overcome. Combined with MEC-based algorithm software, fundamental phase actuation actions can be utilized to balance the traffic demand of different movements [7, 8]. Regarding targets of the real-time TSP algorithm with MEC and CV technology, there are two primary concerns: the phase control strategy for the multidirectional request problem [9] and the minimization of delay [10].

As for the first aspect, the first-in-first-serve (FIFS) policy was firstly applied to resolve conflicting TSP requests by granting priority to the first arrival bus with a request traditionally. However, the performance of the FIFS policy may even cause performance to retrogress with the increase in traffic volume [11].

Subsequently, some rule-based studies have been designed to resolve conflicting TSP requests. These algorithms classify conflicting request issues on a case-by-case basis during each cycle in accordance with the current intersection operation, and through collecting priority requests from conflicting phases, the algorithm outputs the candidate phase as the next priority phase with decision-making mechanisms [9, 10]. There is a rule-based TSP algorithm proposed to define a lot of initialization phase allocation rules according to driving behaviour, such as free flow and car-following, then, taking bus travel time as the objection, redeveloping the timing scheme to ensure selection of the most appropriate TSP plan by comparing bus travel time in the conflict phase. Even though simulation results show that this TSP method effectively improved both the transit bus and general traffic operations against an active TSP strategy,it is difficult to get an optimized result because of those split rules adopted by this method [12]. An analytical rule-based approach to the real-time TSP system for isolated intersections takes the minimum person delay of approach as the decision-making basis due to green extension and red truncation actions [13]. A heuristic algorithm is proposed to achieve near optimal signal timing through transforming all simultaneous requests problems into an s-t network cutting process; microscopic simulation shows bus efficiency improvement while not obvious promotion in vehicle delay compared to exact mathematical programming methods [7].

With the application of programming methods, a great number of studies have shown that intersection efficiency, bus delay, and social vehicle delay, even person delay could be simultaneously improved to varying degrees. These methods are demonstrated to optimize the objection function and the serving sequence by accommodating conflicting requests as well as corresponding signal timings by minimizing delay with consideration of phase sequence, queue dynamics, and delay evaluation constraints [14, 15]. For example, a binary mixed integer linear programming method takes both fixed sequence and person delay into consideration to decrease average person delay [14]. An integer linear programming method is used to optimize an object, including the maximum priority effect and minimum time deviations for nontransit phases. The delay migration time parameters of coordinated phases are further presented for establishing the constraints [15]. A bi-level mixed integer liner programming TSP model whose goal is to optimize intersection efficiency subjects to delay restriction and queue clearance [16]. A traffic-responsive signal control system is presented for signal priority on conflicting transit routes. They provided signal timings that minimized the total person delay of an intersection and allocated weights to the vehicles based on their occupancy [17]. However, these programming algorithms almost regard the priority level of transit buses as the same, which may have potential that can still be improved [18].

To distinguish priority level, some scholars proposed an optimization model to measure the priority level association with transit modes, occupancy, bus routes, and schedule [19–21]. A request-based mixed-integer linear programming model is formulated that explicitly accommodates multiple priority requests from different modes of vehicles, provides signal timings that minimize the total person delay of an intersection, and allocates weights to vehicles only based on their occupancy [22]. Another mixed-integer linear programming model is formulated with subjecting to the real-world constraints for bus rapid transit schedule optimization by minimizing the travel time; in this model, the schedule at

each bus stop and the signal priority control are simultaneously optimized at intersections along the bus rapid line [23]. A priority system involves red truncation and green extension, which determine the weighted priority of buses and social vehicles based on the simplified liner and quadratic arrival and departure curves [24]. For a critical condition, there may be too many social vehicles and few transit buses for a certain movement, and the corresponding phase may not be given higher priority authority than the movement with more transit buses and fewer social vehicles, or it will result in efficiency being lost. Under this condition, it is necessary to measure the dynamic priority weight of individual vehicles to maximize intersection efficiency.

As for the second aspect, some scholars have put forward numerical solutions for the minimum delay; their objects are mainly to figure out the phase control strategy for delay reduction [25]. Part of these scholars selected per person delay, total delay, or average vehicle delay as the objective function with application of the liner programming algorithm, and both simulation experiments and field tests found that they could reduce transit bus delay up to 85% [25, 26]. However, to achieve better performance, these methods need more flexible signal control features to support green re-allocation, including phase split, phase rotation, or green truncation, which may cause control system chaos. Other authors present an approach from the perspective of engineering applications [27, 28]. They paid attention to mining the value of application layer message data like vehicle location and speed in basic safety messages, traffic light state and time to change in signal phase and time messages, trying to find out the direct relationship between objects and these arguments. The rest of the authors construct delay optimization relation models with bus occupancy [29].

In general, even though these methods decrease total transit bus delay, almost all of them neglected the impacts on social vehicle delay for the modelling process so as to be inadequate to maximize intersection efficiency, and due to the complex solving procedure, these types of algorithms may lose effectiveness without the superior system. What is more, few authors establish a transit bus targeted priority weight function in individual vehicles to measure traffic demand better or give an insight into the dynamics of priority weights and relationships among the variables involved. This is valuable for developing a new class of bus priority solutions that are optimal or near-optimal.

In order to fill these gaps, this paper takes full advantage of high-resolution trajectory data of transit buses and arrival flow distribution information that has been postprocessed to establish an easily solvable MEC-based signal control model for the purpose of a swift solving process. In this model, a TTOC-correlation unified dynamic priority weight function is built for measuring single-vehicle priority weight, and an aggregated weighted dynamic priority weight function is derived with consideration of transit buses and social vehicles' arrival patterns to measure the dynamic traffic demand of each movement. The contributions of this work are given as follows:

Firstly, a dynamic priority weight (DPW) model is proposed that is relative to TTOC with consideration of transportation modes and passenger occupancy. There are two functions in this model: one is the unified dynamic priority weight function, which is used to calculate single-vehicle DPW value; the other is the aggregated weighted dynamic priority weight function, which is used to calculate the aggregated weighted dynamic priority weight value of each phase. The aggregated weighted DPW value here represents the right-of-way of one phase; once it reaches the highest level, phase switch prerequisite conditions will be satisfied.

Secondly, a conflicting request resolution control method to actuate the next candidate priority phase for the multidirectional priority request resolution problem is also proposed. Considering the vehicular waiting starvation condition, the phase with the maximum aggregated weighted DPW value is selected as the next candidate priority phase based on the value maximization principle.

The rest of this paper is organized as follows: first of all, the problem is defined with scenarios, a declaration is made, and the main idea is introduced. Then, a dynamic priority weight methodology containing the framework is presented for the modelling process of right of way for each phase, single-vehicle, and aggregated DPW function establishment processes based on case segmentation. Subsequently, a phase switch strategy for multidirectional request resolution control problem is proposed. After that, a numerical simulation is conducted to verify the single-vehicle DPW value variation rule with TTOC, and comparative analysis, simulation experimental, and field tests are carried out for the performance benefits evaluation of the DPW model-based traffic signal control method. The last section is the conclusion.

2. Problem Definition

The modern urban transportation network is composed of multiple travel modes, including general social vehicles (trucks, motorbikes, commercial, and private cars), emergency vehicles, and transit buses. Since the wide distribution of transit buses has a strong demand for right-of-way, the research issue raised in this paper is to resolve multi-directional priority requests at isolated signalized intersections by measuring the total priority weight value of queued vehicles. Three typical traffic light state and TTOC-based scenarios are abstracted by different phase conditions.

As shown in Figure 1(a), the three pictures on the left depict green, red, and yellow traffic light scenarios with a certain TTOC, e.g., 2 seconds, when a transit bus approaches the intersection. The green and yellow traffic light scenarios represent vehicle arrival during the effective green of the current phase, while the red traffic light scenario represents the vehicle arrival during effective green of the conflict phase. The picture on the right depicts the scenario of connected transit buses (yellow rectangle) and social vehicles (black wireframe rectangle) arriving from multiple directions at the same time, in which a multidirectional priority request resolution problem under mixed traffic conditions will be caused.

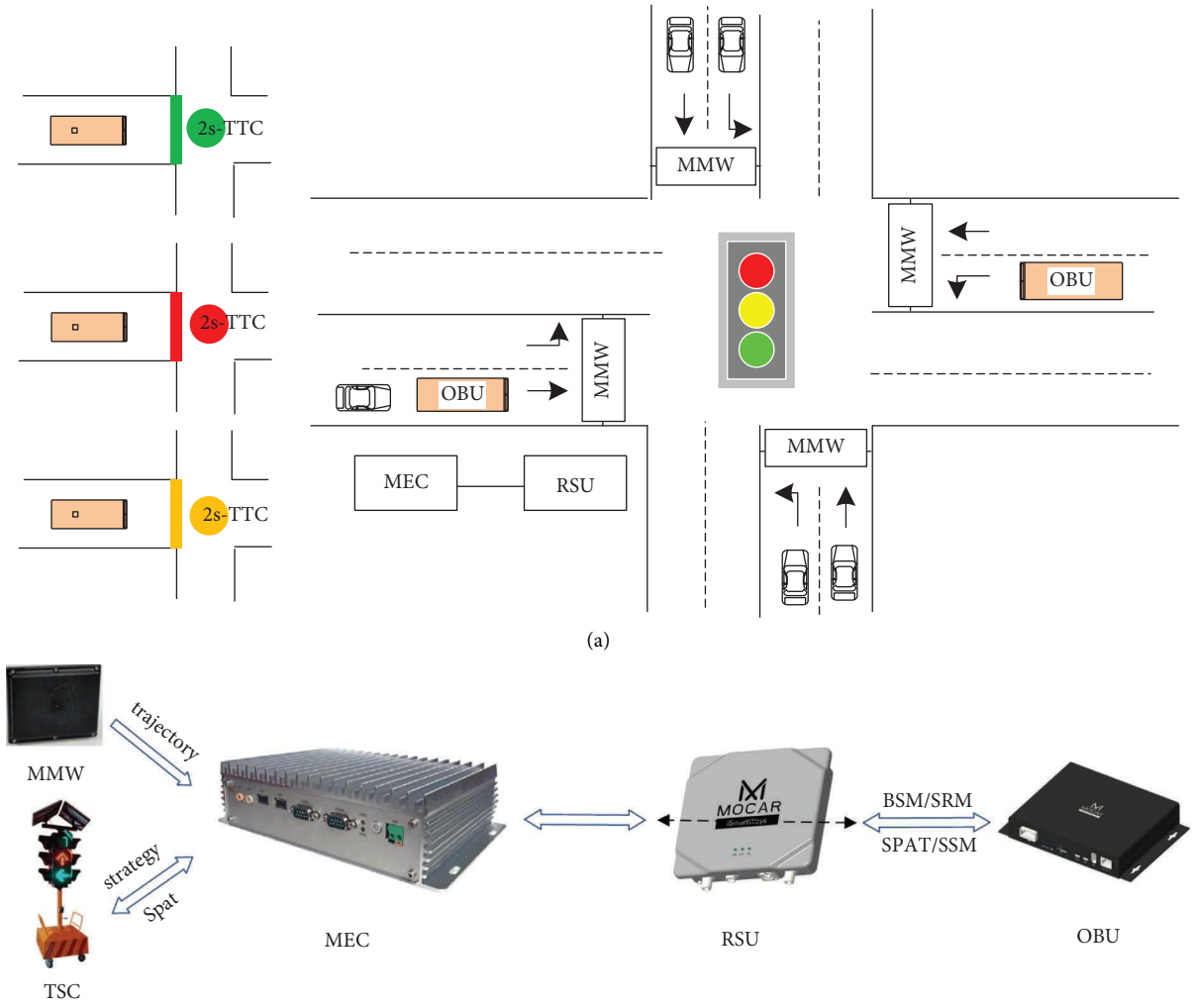

Figure 1: Problem definition. (a) Multidirectional priority request resolution problem under mixed traffic conditions. (b) Information exchange process.

As shown in Figure 1(b), those transit buses equipped with an onboard unit (OBU) can transmit high-resolution trajectory data with a basic safety message (BSM) and priority request data with a signal request message (SRM) to the roadside unit (RSU) through V2I communication, while the RSU broadcasts a signal status message and a signal phase and timing (SPAT) message that carry information about the collection of pending or active priority requests, traffic light state, and time to change all phases. Millimeter-wave radar (MMW) can obtain trajectory data of arrival vehicles, the traffic signal control device (TSC) provides a control strategy interface, MEC acts as an information interaction node that is connected with MMW, RSU, and TSC by optical fiber. All data can simultaneously be delivered to MEC and act as input parameters.

During the process of system operation, the arrival transit buses of different traffic movements will continuously broadcast BSM and SRM, and RSU parse message packets and send trajectory and priority request data to MEC if messages are received. At the same time, both MMW and TSC will send relevant trajectory and signal timing data to MEC. Then, the algorithm outputs the signal control strategy, on the one hand, to actuate traffic light change so that vehicles arriving at the intersection adjust their driving strategies to respond to the new signal timing scheme; on the other hand, to be encapsulated into a signal status message (SSM) and SPAT, the transit bus receiving the message changes or maintains the current motion state to respond to the new phase switch strategy. Besides connected transit buses, social vehicles do not have communication capacity; their spatial-temporal position and velocity information are not available for us to estimate the distribution. We regard social vehicles' arrival as normal distribution and the headway as constant, and we assume that the dissipation rate is equal to the saturation rate once the traffic light turns green.

3. Methodology: Dynamic Priority Weight Model and Resolution Control

In this section, we build a dynamic competitive priority model based on TTOC to measure the priority weight of arrival vehicles. The section is organized as follows: Section

3.1 introduces the framework of the proposed method. Sections 3.2 and 3.3 introduce the priority weight calculation function for individual vehicles and the total priority weight calculation for each movement, respectively. Section 3.4 introduces the resolution control method for phase switching.

3.1. Framework. As for the multi-directional priority request resolution control problem, arriving vehicles from major traffic movements with the strongest demand for right-of-way will be blocked at the intersection during the red interval, while, the other traffic movement, which only has a lower demand, is given the green light to discharge. For satisfying traffic demand better under this situation, an optimized three-stage framework is set up.

As shown in Figure 2, in the first stage, we distinguish two cases according to the traffic light state in the direction of the vehicle arriving: vehicle arrival during the effective green of both the current and the conflicting phase. A unified dynamic priority weight function is constructed to establish the relationship between individual vehicle priority weight of each movement and TTOC, by the way, to ensure that the number of queueing transit buses dissipates as much as possible with consideration of the actual green or red interval. The output of this function, the single-vehicle DPW value, is used to measure the priority weight of an individual vehicle with one passenger for two cases.

In the second stage, an aggregated weighted DPW function is subsequently established to measure the total priority weight of arriving vehicles for each movement by aggregating the single-vehicle DPW value for the same case. The output of this function, the aggregated weighted DPW value, represents the competitiveness defeating other phases to gain priority; the greater the aggregated weighted DPW value, the stronger the right-of-way competitiveness of the phase is.

The third stage, resolution control for conflicting requests, is the method to coordinate conflict requests, including aging timer design to avoid starvation conditions happening and aggregated priority weight based on a value maximization signal control strategy.

The notation in Table 1 is used to define the following proposed algorithm.

3.2. Unified Dynamic Priority Weight Function. As the first stage of the framework, this subsection explains the derivation process of the unified dynamic priority weight function. Figure 3 describes the unified dynamic weight function curve for two cases of vehicle arrival during the effective green of the conflict phase and the current phase.

As shown in Figure 3, it gives a description of the linear variation relation curve of the unified DPW function of the priority request phase. The vertical intercept, the dimensionless single-vehicle DPW value, varies within the range of 0–1 related to the TTOC of the priority request phase, and the horizontal axis intercept means the actual red and green intervals of the requesting phase with consideration of red truncation and green extension.

To be more specific, the left view of Figure 3(a) illustrates that the red interval cuts for truncated seconds if a request is received at the timestamp of a certain TTOC. The truncated seconds are represented by a red hollow region, and the actual red interval is represented by a red solid region covering the horizontal axis, so the dashed line of the function will substitute for the solid line. In the left view of Figure 3(b), the unified dynamic priority weight function curve can be separated into two parts based on single-vehicle DPW value: the constant part expresses the maximum DPW value if green TTOC is less than the minimum green interval, and the liner variation part expresses the value varying from green TTOC if green is consumed with more than the minimum green interval. In addition, green extension at the timestamp of a certain TTOC makes the green interval extend for seconds so that the function curve moves parallel to the right from the dashed line to the solid line with extra extended seconds. Besides, the right view of Figures 3(a) and 3(b) is utilized to analyze actual red interval and actual green interval variation with split control, which will be given detailed instructions in the following subsections.

3.2.1. Vehicle Arrival during the Effective Green of the Conflict Phase. In this case, when a vehicle arrives at the intersection, the traffic light state of the conflict phase is green, and inversely, the traffic light of the current requesting phase is red. From Figure 3(a), it can be seen that the single-vehicle DPW value will be linearly dependent on TTOC. We set the red interval with r and the unified dynamic priority weight function without red truncation (the dash line) can be described with the following liner equation:

$$f_s(t_{\text{ttoc}}) = 1 - \frac{t_{\text{ttoc}}}{r}, 0 \le t_{\text{ttoc}} \le r. \tag{1}$$

According to the minimum green interval protective principle, whether the latest request is responded to depend on the green TTOC of the conflict phase when the request is received; if the deviation between TTOC and the maximum green interval is less than the minimum green interval, the conflict phase will not be forced off soon. So, based on the remaining green time periods of conflict phase, it should be divided into two situations, consumed green time periods of conflict phase less than the minimum green interval, and conflict phase kept green longer than the minimum green interval.

The right view of Figure 3(a) describes the actual red interval of the current requesting phase if the request is received at the timestamp of TTOC, which is equal to t_{ttoc}^{lr} for the first situation. In this situation, green TTOC of conflict phase satisfying with a relational expression of $g_{\max}^{\text{con}} - g_{\min}^{\text{con}} < t_{\text{ttoc}}^{\text{con}} \le g_{\max}^{\text{con}}$, the remaining green time of conflict phase becomes as follows:

$$g_k^{\text{con}} = g_{\min}^{\text{con}} + y^{\text{con}} - (g_{\max}^{\text{con}} - t_{\text{ttoc}}^{\text{con}}). \tag{2}$$

Correspondingly, the priority-requesting phase keeps turning red for g_k^{con} seconds before turning green (pink

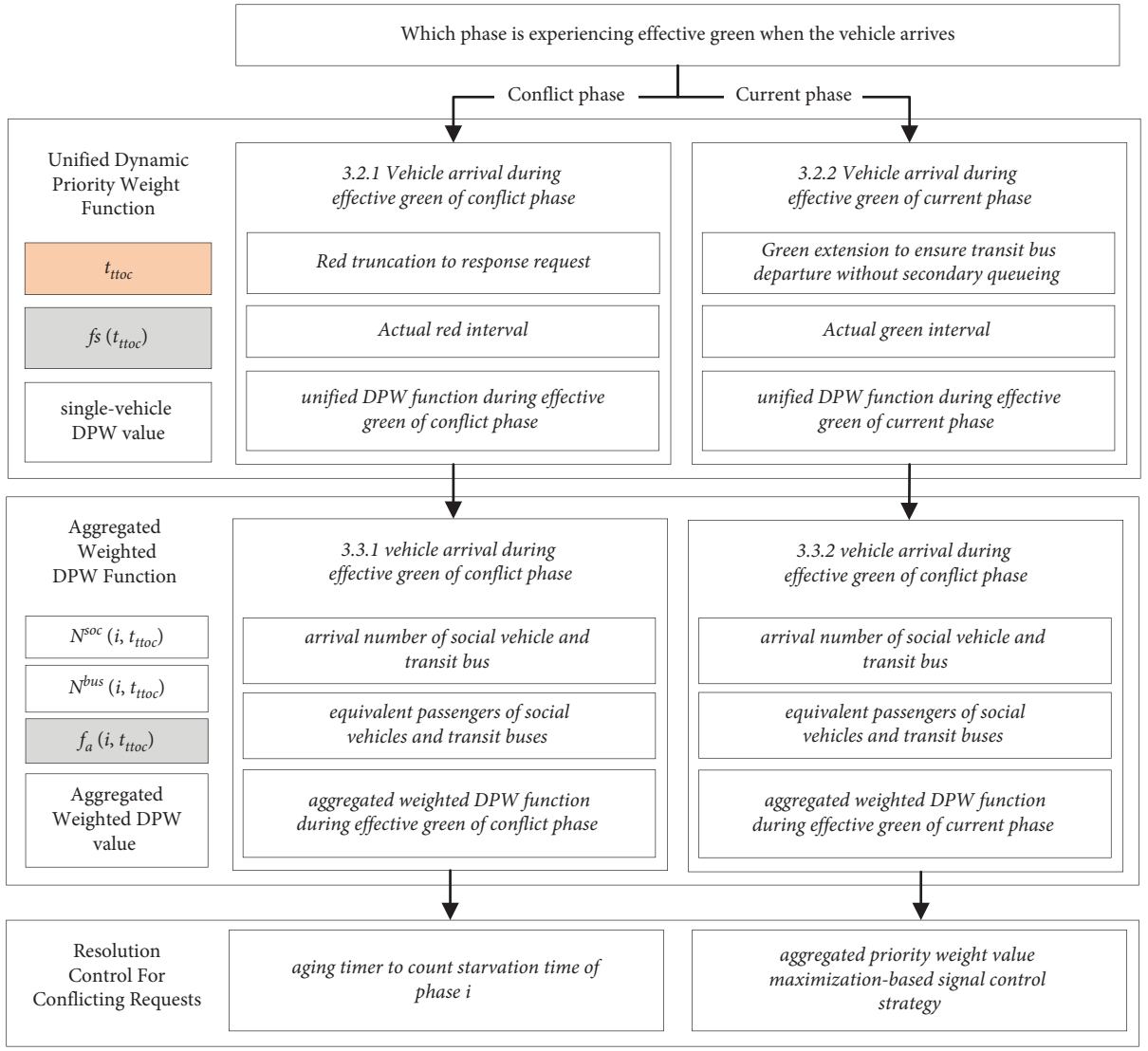

Figure 2: The framework of the proposed conception.

Table 1: Notation table.

Name	Description
t_{ttoc}	Time to change the current green phase
t_{ttoc}^{lr}	Time to change the current phase when the latest request is received
$t_{\text{ttoc}}^{\text{con}}$	Time to change the conflict phase when the latest request is received
r	Red interval
y	Yellow interval
$g_{\text{max}}^{\text{con}}$	Maximum green interval of conflict phase
$g_{\text{min}}^{\text{con}}$	Minimum green interval of conflict phase
g_{max}	Maximum green interval of current phase
g_{min}	Minimum green interval of current phase
g_k^{con}	Red continued seconds for the priority requesting phase before turning to green
δ	Dirac delta function
Δg	Extended green seconds
Δg_1	Part of green extension seconds to guarantee the bus passing through the intersection
Δg_2	Part of green extension seconds to discharge queued vehicles with avoidance of secondary queueing
S	Queueing vehicle departure flow speed
d_{lr}	the distance to stop bar of the vehicle at the tail of the queue
$ar\ (t_{\text{ttoc}}^{lr})$	Vehicle arrival flow speed pattern function relation with t_{ttoc}^{lr}
$\text{sar}\ (i)$	Social vehicle arrival flow speed pattern function relation of phase i

Table 1: Continued.

Name	Description
i	Phase index
I	Set of phase index
$\mu(i)$	Expectation of vehicle arrival flow speed pattern of phase i
$\sigma(i)$	Standard deviation of vehicle arrival flow speed pattern of phase i
$f_s(t_{\text{ttoc}})$	Unified dynamic priority weight function for single-vehicle DPW value calculation relation with t_{ttoc}
$f_s(i, t_{\text{ttoc}})$	Unified dynamic priority weight function for single-vehicle DPW value calculation relation with t_{ttoc} of phase i
$f_a^{\text{bus}}(i, t_{\text{ttoc}})$	Aggregated weighted dynamic priority weight function of transit bus for aggregated weighted DPW value calculation relation with t_{ttoc} of phase i
$f_a^{\text{soc}}(i, t_{\text{ttoc}})$	Aggregated weighted dynamic priority weight function of social vehicle for aggregated weighted DPW value calculation relation with t_{ttoc} of phase i
$f_a(i, t_{\text{ttoc}})$	Aggregated weighted dynamic priority weight function for aggregated weighted DPW value calculation relation with t_{ttoc} of phase i
$N^{\text{bus}}(i, t_{\text{ttoc}})$	Arrival transit bus number
$N^{\text{soc}}(i, t_{\text{ttoc}})$	Arrival social vehicle number
ps	Phase state, "1" and "2" represent vehicle arrival during effective green of current phase and conflict phase, respectively
φ	Passenger occupancy of transit bus
$t_{\text{wait}}(i)$	The waiting timer of phase i
$\text{timer}(i)$	Aging timer to count starvation time of phase i
TIMER	Waiting time threshold
t_{eta}	Estimated time for the arrival of the transit bus at the tail of the queue
d	Distance to stop bar of the transit bus at the tail of the queue

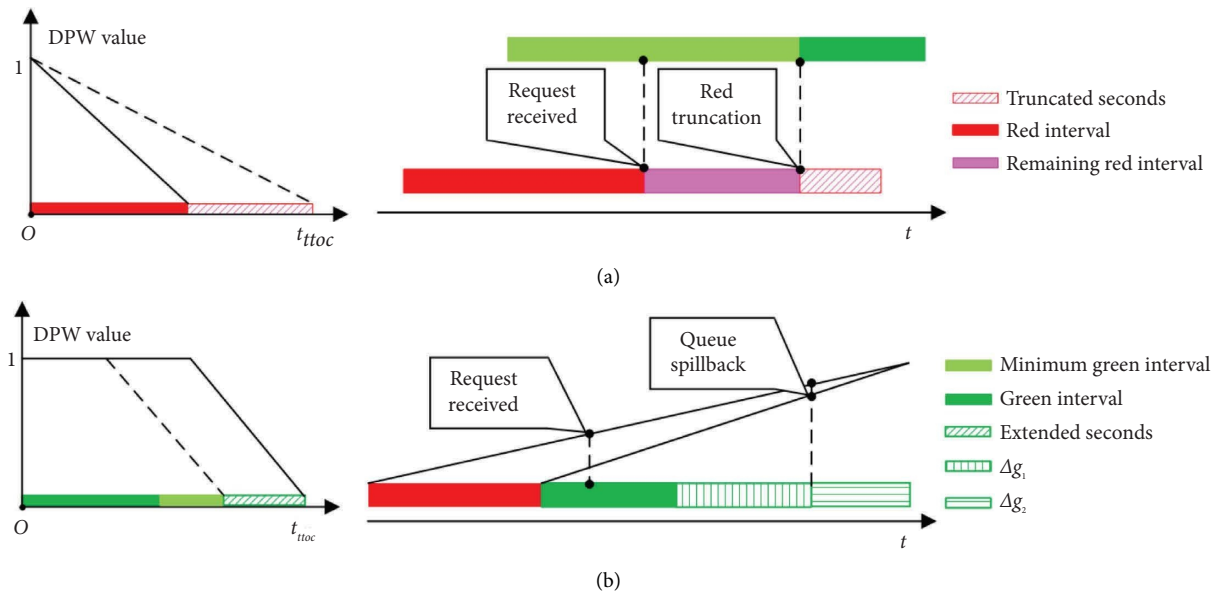

Figure 3: The unified DPW function curve for two cases of vehicle arrival during the effective green of the conflict and the current phase. (a) Effective green of the conflict phase. (b) Effective green of the current phase.

region), which results that the actual red interval of the requesting phase becomes $r_a = r - t_{\text{ttoc}}^{lr} + g_k^{\text{con}}$.

For the second situation, green TTOC of the conflict phase satisfies with a relational expression of $0 \le t_{\text{ttoc}}^{\text{con}} \le g_{\max}^{\text{con}} - g_{\min}^{\text{con}}$, phase switch executes as soon as possible for the reason of experienced minimum green time periods. Ignoring transition delay, the actual red interval of the current requesting phase will be $r - t_{\text{ttoc}}^{lr}$. Combining with the impacts that split control has on the actual red interval of the requesting phase, we can infer a unified DPW function of the case about vehicle arrival during the effective green of the conflict phase into the following equation:

$$f_s(t_{\text{ttoc}}) = \begin{cases} 1 - \dfrac{t_{\text{ttoc}} - t_{\text{ttoc}}^{lr} + g_k^{\text{con}}}{r - t_{\text{ttoc}}^{lr} + g_k^{\text{con}}}, & if\ g_{\max}^{\text{con}} - g_{\min}^{\text{con}} < t_{\text{ttoc}}^{\text{con}} \le g_{\max}^{\text{con}}, 0 < t_{\text{ttoc}} < r) \\ 1 - \dfrac{t_{\text{ttoc}} - t_{\text{ttoc}}^{lr}}{r - t_{\text{ttoc}}^{lr}}, & if\ 0 \le t_{\text{ttoc}}^{\text{con}} \le g_{\max}^{\text{con}} - g_{\min}^{\text{con}}, 0 < t_{\text{ttoc}} < r), \end{cases} \tag{3}$$

where the curve corresponds to the solid line in the left view of Figure 3(a), and the output is the single-vehicle DPW value for this case.

3.2.2. Vehicle Arrival during the Effective Green of the Current Phase. In this case, when a vehicle arrives at the intersection, the traffic light state of the current phase is green, and the single-vehicle DPW value is only relative to the green TTOC of the current phase. Without phase control, the effective green interval of the current phase equals the green interval ($g_{\max}$) plus the yellow interval (y), and the equivalent minimum green interval is $g_{\min} + y$. From the left view of Figure 3(b), it can be seen that the DPW function gets its maximum value when TTOC is less than the minimum green interval, while the value liner drops if TTOC becomes more (the dash line). Introducing the Dirac Delta function $\delta(t_{\text{ttoc}} - g_{\min} - y)$, we can express the unified DPW function as the following equation:

$$f_s(t_{\text{ttoc}}) = 1 - \frac{t_{\text{ttoc}} - (g_{\min} + y)}{g_{\max} - (g_{\min} + y)}\delta(t_{\text{ttoc}} - g_{\min} - y), 0 \langle t_{\text{ttoc}} \langle g_{\max}, \tag{4}$$

where t_{ttoc} in the fractional numerator is equivalent to the remaining green time. Since split control extends the actual effective green interval with green hold actions, for the extended green seconds Δg, on the one hand, it should ensure that transit buses pass through the intersection during the current signal cycle; on the other hand, it should ensure to avoid the occurrence of queue spillback as much as possible. For this reason, Δg is relative with TTOC when the latest request is received, formulated as $\Delta g = \Delta g(t^{lr}_{\text{ttoc}})$, and the remaining green time and actual effective green interval become $[t^{lr}_{\text{ttoc}} + \Delta g(t^{lr}_{\text{ttoc}})]$ and $g_{\max} + y + \Delta g(t^{lr}_{\text{ttoc}})$.

To explain the composition of Δg, the right view of Figure 3(b) illustrates a queue dissipation process during the green interval. Assuming RSU receives the latest request with a timestamp for a certain TTOC donated by t^{lr}_{ttoc}, in order to ensure there are no other vehicles blocked in the intersection before the traffic light turns to red, Δg should consist of two parts. One of them, $\Delta g_1(t^{lr}_{\text{ttoc}})$, is to guarantee the transit bus passing through the intersection; another one of them, $\Delta g_2(t^{lr}_{\text{ttoc}})$, is to be added to discharge other queued vehicles. Because the locations of transit buses and stop lines can be accessed, the distance to the stop bar (d_{lr}) of the vehicle at the tail of the queue, which represents the updated queue length, can be calculated. Combined with saturation flow speed $S$and expectation of arrival flow speed $E[ar(t^{lr}_{\text{ttoc}})]$, $\Delta g(t^{lr}_{\text{ttoc}})$ can be expressed as follows:

$$\Delta g\left(t^{lr}_{\text{ttoc}}\right) = \frac{d_{lr}}{S - E\left[ar\left(t^{lr}_{\text{ttoc}}\right)\right]} - t^{lr}_{\text{ttoc}}, 0 \langle t^{lr}_{\text{ttoc}} \langle g_{\max}(6), \tag{5}$$

where $ar(t^{lr}_{\text{ttoc}})$ denotes the vehicle arrival flow speed pattern function that is normally distributed with a constant mean value and standard deviation during a period, whether in peak hours or off-peak hours [6]. Bring equation (5) into equation (4) and using t_{ttoc} instead of t^{lr}_{ttoc}, we can derive the unified DPW function of vehicle arrival during the effective green of the current phase as the following equation:

$$f_s(t_{\text{ttoc}}) = 1 - \frac{\Delta g(t_{\text{ttoc}}) + t_{\text{ttoc}} - (g_{\min} + y)}{[\Delta g(t_{\text{ttoc}}) + g_{\max}] - (g_{\min} + y)}\delta(t_{\text{ttoc}} - g_{\min} - y), 0 \langle t_{\text{ttoc}} \langle g_{\max}, \tag{6}$$

where the curve corresponds to the solid line of the left view in Figure 3(b), and the output is the single-vehicle DPW value for this case.

3.3. Aggregated Weighted Dynamic Priority Weight Function. In this section, the aggregated weighted dynamic priority weight function ($f_a(i, t_{\text{ttoc}})$) is derived to measure the total priority weight of one phase, which is made up of two parts differentiated by traffic modes, aggregated weighted DPW function of $N^{\text{bus}}(i)$ transit buses of phase i ($f^{\text{bus}}_a(i, t_{\text{ttoc}})$), and aggregated weighted DPW function of $N^{\text{soc}}(i)$ social vehicles in phase i ($f^{\text{soc}}_a(i, t_{\text{ttoc}})$).

Meanwhile, we are also aiming at establishing a weighting function related to the number of passengers; the average passenger occupancy ($\varphi, \varphi \geq 1$) factor is introduced into the aggregated weighted DPW function expressed as follows:

$$f^{\text{bus}}_a(i, t_{\text{ttoc}}) = \sum_{N^{\text{bus}}\left(i, t_{\text{ttoc}}\right)} f_s(i, t_{\text{ttoc}}), \tag{7a}$$

$$f^{\text{soc}}_a(i, t_{\text{ttoc}}) = \sum_{N^{\text{soc}}\left(i, t_{\text{ttoc}}\right)} f_s(i, t_{\text{ttoc}}), \tag{7b}$$

$$f_a(i, t_{\text{ttoc}}) = \varphi * f^{\text{bus}}_a(i, t_{\text{ttoc}}) + f^{\text{soc}}_a(i, t_{\text{ttoc}}). \tag{7c}$$

To be more specific, in equation (7a), $f^{\text{bus}}_a(i, t_{\text{ttoc}})$ is a summation process by $f_s(i, t_{\text{ttoc}})$, which results that RSU can persistently record requests for the identification of transit buses. In (7b), social vehicle arrival pattern distribution is substituted to calculate the arrival number $N^{\text{soc}}(i, t_{\text{ttoc}})$.

Adding $f_a^{\text{bus}}(i, t_{\text{ttoc}})$ and $f_a^{\text{soc}}(i, t_{\text{ttoc}})$, the purposeful function $f_a(i, t_{\text{ttoc}})$ can be derived in (7c), the output of this function represents the aggregated weighted DPW value of one phase. What's more, inheriting the classification principle of the unified DPW function aforementioned in the last subsection, two cases of vehicle arrival during the effective green of conflict phase and current phase are also taken into consideration to derive aggregated DPW function in the following paragraphs.

3.3.1. Aggregated Weighted DPW Function for Vehicle Arrival during Effective Green of Conflict Phase. In this case, the traffic light is red when vehicles arrival, which results to $ps = 2$. Aggregated weighted DPW function can be figured out with three steps according to equations (7a)–(7c). For the first step, combined with the arrival bus number counted by receiving requests and unified DPW function $(f_s(i, t_{\text{ttoc}}), ps = 2)$, $f_a^{\text{bus}}(i, t_{\text{ttoc}})$ can be expressed as follows:

$$f_a^{\text{bus}}(i, t_{\text{ttoc}}) = N^{\text{bus}}(i, t_{\text{ttoc}}) * f_s(i, t_{\text{ttoc}}), ps = 2. \tag{8}$$

For the second step, assuming the vehicle arrival flow pattern follows a normal distribution as $ar \sim N(\mu, \sigma)$, where μ and σ are the expectation and standard derivation of arrival flow speed, and the average penetration rate of the social vehicle is λ, then, social vehicle arrival flow pattern of phase i will be distributed as $\text{sar}(i) \sim N(\lambda * \mu(i), \sigma(i))$. Therefore, the social vehicle arrival number during the actual red interval can be expressed as follows:

$$N^{\text{soc}}(i, t_{\text{ttoc}}) = \int_0^{r_a} 1/\sqrt{2\pi\sigma(i)}e^{-(t-\lambda*\mu(i))^2/2\sigma(i)^2}dt \ , 0 \langle t_{\text{ttoc}} \langle r). \tag{9}$$

For the third step, by multiplying the average passenger occupancy and unified DPW function, aggregated weighted DPW function for vehicle arrival during effective green of conflict phase case in equation (7c) transforms to the following:

$$f_a(i, t_{ttoc}) = \underbrace{f_s(i, t_{ttoc})}_{\substack{single-vehicle \\ DPW\ value}} * \left[\underbrace{\varphi N^{bus}(i, t_{ttoc})}_{\substack{equivalent\ transit \\ bus\ passenger}} + \underbrace{\int_0^{r_a} \frac{1}{\sqrt{2\pi\sigma(i)}} e^{-\frac{(t-\lambda*\mu(i))^2}{2\sigma(i)^2}} dt}_{\substack{equivalent\ social \\ vehicle\ passenger}} \right], if\ ps = 2,\ 0 < t_{ttoc} < r \tag{10}$$

$$f_s(i, t_{ttoc}) = \begin{cases} \left(1 - \dfrac{t_{ttoc} - t_{ttoc}^{lr} + g_k^{con}}{r - t_{ttoc}^{lr} + g_k^{con}}\right), \ g_{\max}^{con} - g_{\min}^{con} < t_{ttoc}^{con} \le g_{\max}^{con} \\ \left(1 - \dfrac{t_{ttoc} - t_{ttoc}^{lr}}{r - t_{ttoc}^{lr}}\right), 0 \le t_{ttoc}^{con} \le g_{\max}^{con} - g_{\min}^{con} \end{cases},$$

where there are three critical components: equivalent transit bus passenger number, equivalent social vehicle passenger, and single-vehicle DPW value.

3.3.2. Aggregated Weighted DPW Function for Vehicle Arrival during Effective Green of Current Phase. The derivative process of aggregated weighted DPW function for this case is similar to that of the first case. Equations (7a)–(7c) are transformed to aggregated weighted DPW function for this case. Specifically, the first step, combined with $N^{\text{bus}}(i, t_{\text{ttoc}})$ and unified DPW function $(f_s(i, t_{\text{ttoc}}), ps = 1)$, $f_a^{\text{bus}}(i, t_{\text{ttoc}})$ can be expressed as follows:

$$f_a^{\text{bus}}(i, t_{\text{ttoc}}) = N^{\text{bus}}(i, t_{\text{ttoc}}) * f_s(i, t_{\text{ttoc}}), ps = 1. \tag{11}$$

For the second step, since queueing social vehicle number is composed of two parts: social vehicle arrival number during the actual red and green interval, and social vehicle departure number during the actual green interval. According to the vehicular arrival distribution function and queue dissipation speed, the updated queueing social vehicle

number by the timestamp of receiving the latest request can be expressed as follows:

$$N^{\text{soc}}(i,t_{\text{ttoc}}) = \underbrace{\int_0^{r+g_{\max}-t_{ttoc}} 1/\sqrt{2\pi\sigma(i)}e^{-(t-\lambda*\mu(i))^2/2\sigma(i)^2}dt}_{\text{arrival number}} - \underbrace{S*(g_{\max}-t_{\text{ttoc}})}_{\text{departure number}}, 0\langle t_{ttoc}\langle g_{\max}. \tag{12}$$

For the third step, multiplying the average passenger occupancy by the unified DPW function, aggregated weighted DPW function for vehicle arrival during effective green of the current phase case can be derived. It also contains three critical components, equivalent transit bus passenger number, equivalent social vehicle passenger, and single-vehicle DPW value, which is exactly the same as equation (10).

$$f_a(i,t_{ttoc}) = \underbrace{f_s(i,t_{\text{ttoc}})}_{\substack{\text{single-vehicle}\\ DPW\text{value}}} * \left[\underbrace{\varphi N^{\text{bus}}(i,t_{\text{ttoc}})}_{\substack{\text{equivalenttransit}\\ \text{buspassenger}}} + \underbrace{\int_0^{r+g_{\max}-t_{\text{ttoc}}} 1/\sqrt{2\pi\sigma(i)}\, e^{-(t-\lambda*\mu(i))^2/2\sigma(i)^2}dt - S*(g_{\max}-t_{\text{ttoc}})}_{\text{equivalentsocialvehiclepassenger}}\right] \tag{13}$$

$$f_s(i,t_{\text{ttoc}}) = 1 - \frac{d_{lr}/\{S-E[ar(t_{\text{ttoc}})]\} + t_{\text{ttoc}} - (g_{\max}+y)}{d_{lr}/\{S-E[ar(t_{\text{ttoc}})]\} + (g_{\max}-g_{\min})} * \delta(t_{\text{ttoc}} - g_{\min} - y), if\ ps = 1, 0\langle t_{\text{ttoc}}\langle g_{\max}.$$

3.4. Resolution Control for Conflicting Requests. As the second stage of the framework, in this section, a phase switch strategy is designed to make the next priority phase actuating decision for multi-directional conflicting priority request resolution control. Based on the value maximization principle, the phase of maximum aggregated weighted DPW value is selected as the candidate's next priority phase.

3.4.1. Starvation Condition. The phase with lower aggregated weighted DPW value may continuously lose the right-of-way, if there is only a small number of arrival vehicles for a certain traffic movement, a starvation condition is inevitably caused for the reason of the long waiting time of those arrived vehicles. To avoid this starvation condition happening, a waiting timer $t_{\text{wait}}(i)$ with an initialization value of 1 to count waiting seconds and a binary aging timer $\text{timer}(i,t_{\text{wait}}(i))$ with values of 1 and 100 respectively of phase i are employed. Once a vehicle arrives at the intersection, the waiting timer starts counting and adding one per second, when the waiting timer exceeds the predefined threshold TIMER, the aging timer will switch from 1 to 100 so that aggregated weighted DPW value multiplied by the aging timer will be hundred times of the initial one. $\text{timer}(i,t_{\text{wait}}(i))$ is listed as the following equation:

$$\text{timer}(i,t_{\text{wait}}(i)) = \begin{cases} 100, & if\ t_{\text{wait}}(i) \geq \text{TIMER}, \\ 1, & if\ t_{\text{wait}}(i) \langle \text{TIMER}. \end{cases} \tag{14}$$

If a critical movement is served in the next phase, the waiting timer of that phase is reset to 0. To avoid giving the right-of-way to a movement with no vehicle, the reset waiting timer will not restart until a new vehicle arrives.

3.4.2. Phase Switch Strategy. The phase switch strategy contains two components, one is the process of finding the candidate's next phase based on the value maximization principle, and another one is the restrictive condition of the phase switch to guarantee the transit bus pass through the intersection without secondary queueing.

For the first component, the phase which has the maximum aggregated weighted DPW value multiplied by the aging timer will be chosen as the candidate's next priority phase, the equation can be expressed as follows:

$$f(i) = \text{argmax}_i\{\text{timer}(i) \times f_a(i,t_{\text{ttoc}}) | \forall i \in I\}. \tag{15}$$

For the second component, the unified DPW value is likely to increase less for the current phase than that of other conflict phases because of the inconsistent slope of the unified DPW function curve during the effective green of the current phase and conflict phase. In addition, TTOC reduction makes unified DPW value become more, while the number of queueing vehicle decrease with vehicles departure, which has an opposite effect on aggregated weighted DPW value, this inevitably causes uncertainty changes on the total priority weight magnitude relationship among all phases anytime. Both of the two reasons result in the extended seconds not being enough to ensure the transit bus pass through the intersection for the case of vehicle arrival during the effective green of the current phase, for the extended seconds estimated at the timestamp of the transit bus

just approaching to the intersection, it may not be applicable several seconds later. So, if the phase switch action executes without any assurance limitations, the immediately executed phase switch will lead to traffic efficiency loss.

Based on the above analysis, we design a current phase protection mechanism shown in Algorithm 1 to ensure that the transit bus has left the intersection before switching to the candidate's next phase. It has three critical steps: calculate aggregated weighted DPW value of all phases, return the phase of maximum value, and determine whether the returned phase is the green phase. The additional green hold will continue to execute with the right determination result, or the time to arrival of the transit bus at the tail of the queue will be estimated as the minimum necessary waiting time to assure queue clearance before the phase switch. Assuming that queueing vehicle dissipation with saturation flow speed is the same as that expressed in equation (5), then the estimated minimum waiting time becomes the following:

$$t_{\text{eta}} = \frac{d}{S}. \tag{16}$$

4. Evaluation and Analysis

In this section, queuing vehicle number and throughput rate of each movement are evaluated to verify the effectiveness of the DPW model-based signal control method proposed in this paper. It contains (1) a numerical simulation experiment to verify the DPW value variation rule with TTOC, (2) a comparative simulation experiment to evaluate performance benefits with the DPW-based method, and (3) a field test to verify the practical effect and performance comparison with current research.

4.1. Field Test Setup. Figure 4 depicts the intersection orientation, traffic movement, device layout, and signal phase and timing configuration of the field test environment. In Figure 4(a), an isolated signalized intersection crossed by Checheng South Road and Zhushan Lake Avenue, located in Wuhan National Connected Autonomous Vehicle Demonstration Zone, was selected as the experimental site to carry out data collection. It is a two-way, six-lane road with a speed limit of 60 km/h and an undersaturated traffic flow intersection, and each lane corresponds to left-turn movement, through movement, and right movement.

For this intersection, both phase one and phase six are located on Checheng South road, corresponding to through and left-turn movement from southeast to northwest direction, while phase two and phase five are in the opposite direction. Both phase three and phase eight are located on Zhushan Lake Avenue, corresponding to through and left-turn movement from southwest to northeast direction. In contrast, phase four and phase seven are from the northeast.

Data acquisition devices are installed alongside the intersection. There are four millimeter-wave radars on the gantry frame above the stop line, which can collect arrival vehicle trajectory data with meter-level accuracy within the range of 200 m. RSU is also installed for collecting connected transit bus priority request and their trajectory data through V2I communication. Meanwhile, all of these devices are connected with MEC, which is distributed deployment at the intersection.

To examine the DPW model-based signal control method performance influence factor, data collection has been carried out for simulation inputs reference by obtaining necessary signal timing and traffic flow parameters. Fixed timing is shown in Figure 4(b), and general traffic parameters, arrival flow, saturation flow, and transit bus penetration rate of all phases are listed in Table 2. It can be seen from Table 2 that traffic movements of phases one, two, five, and six have distinctly more arrival flow and transit bus penetration than that of Zhushan Lake Avenue. This is because Checheng South Road has prime traffic flow, and there are more bus transit bus operation routes on this road. Furthermore, we assume that passenger occupancy of transit buses is 20. Then we analyze the collected experimental data to complete evaluation works.

4.2. Numerical Simulation Experiment. Numerical simulation is adopted to verify the single-vehicle DPW value variation rule with TTOC. All calculations are conducted with MATLAB based on the parameters in Table 2. We assume that only a single vehicle locates at the stop bar of each movement, and we draw the curve of the single-vehicle DPW value with respect to the TTOC of phases in ring one as shown in Figure 5.

Figure 5(a) depicts the unified DPW function curve with respect to the TTOC of phase one. Curves from left to right represent the relationship between single-vehicle DPW value and TTOC during green and red intervals but priority requests are received at 0 s, 20 s, 40 s, 60 s, and 80 s. Red truncation eventually results in the actual red interval changing to 90 s, 75 s, 50 s, 30 s, and 10 s. During the green interval, the single-vehicle DPW value shows a piecewise linear change from 0 to 1 when TTOC is between maximum green (40 s) and minimum green (10 s). If TTOC is less than the minimum green, the single-vehicle DPW value will remain 1 until the traffic light turns red. During the red interval, that TTOC equal to zero represents a priority request received at the last second, the curve experiences linear growth with TTOC declining. It should be noticed that the priority request received at 20 s-TTOC will not drive red truncation action immediately because of not experiencing the full minimum green duration for phase four. Green holds for another five seconds, and the actual red interval changes to seventy-five seconds for phase one (Figure 4(b)). If a priority request is received at other timestamps, red truncation will lead to the actual red interval being equal to time periods from the timestamp of the maximum red interval to the timestamp of the priority request received, and the single-vehicle DPW value will reach a peak at that time.

Figures 5(b)–5(d) compare the single-vehicle DPW value of four phases in ring one during the green interval of phase one by assuming that certain conflict phase priority requests will have been received at the typical TTOC of phase one. From these three subfigures, we can know that the actual

Require: objective function $f(i)$, t_{ttoc}, $ps(i)$, $N^{\text{bus}}(i, t_{\text{ttoc}})$, $N^{\text{soc}}(i, t_{\text{ttoc}})$, $f_s(i, t_{\text{ttoc}})$, $f_a(i, t_{\text{ttoc}})d$, S, t_{eta}, d_{lr}, Δg

(1) Initialization: $t_{\text{wait}}(i) \leftarrow 0$
(2) **for** $i = 1$: I **do**
(3) Calculate aggregated DPW value for phase i
(4) $ps \leftarrow ps(i)$ #update the traffic light state of the phase
(5) $t_{\text{ttoc}} \leftarrow t_{\text{ttoc}}(i) - 1$ #update TTOC
(6) $t_{\text{wait}}(i) \leftarrow t_{\text{wait}}(i) + 1$# #update waiting time
(7) $f_s \leftarrow f_s(i, t_{\text{ttoc}})$ #update single-vehicle DPW value
(8) $N^{\text{bus}} \leftarrow N^{\text{bus}}(i, t_{\text{ttoc}})$ #update queueing bus number
(9) $N^{\text{soc}} \leftarrow N^{\text{soc}}(i, t_{\text{ttoc}})$ #update queueing social vehicle number
(10) $f_a \leftarrow f_a(i, t_{\text{ttoc}})$ #update aggregated weighted DPW value
(11) timer $\leftarrow$ timer(i) #update aging timers
(12) **end**
(13) $f(i) = \text{argmax}_i\{\text{timer}(i) \times f_a(i, t_{\text{ttoc}}) | \forall i \in I\}$ #update objective phase number
(14) **if** $f(i) \triangleq i$, **then**
(15) $\Delta g \leftarrow d_{lr}/S - E[ar(t^{lr}_{\text{ttoc}})] - t^{lr}_{\text{ttoc}}$ #update green extension for current phase
(16) **else if** $f(i) \neq i$, **then**
(17) $t_{\text{eta}} \leftarrow d/S$ #update waiting time of phase switch
(18) **end**

Algorithm 1: phase switch strategy.

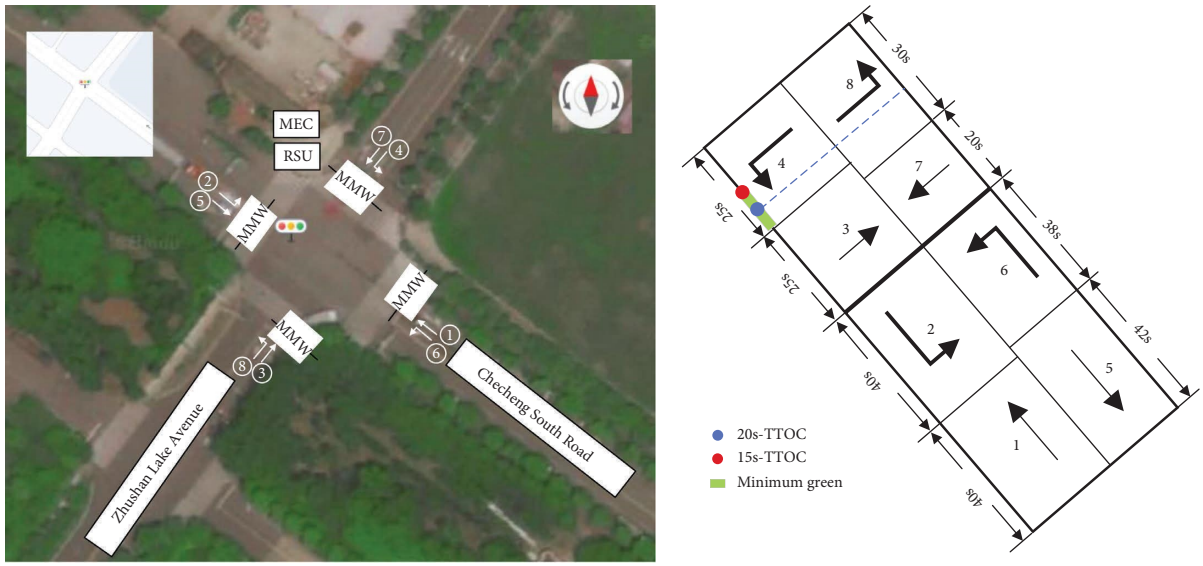

Figure 4: Field test environment. (a) Traffic movement and device layout. (b) Signal phase and timing graph.

Table 2: Fixed timing and traffic parameters.

Phase no.	One	Two	Three	Four	Five	Fix	Seven	Eight
Green interval (s)	40	40	25	25	42	38	20	30
Minimum green (s)	10	10	10	10	10	10	10	10
Red interval (s)	90	90	105	105	88	92	110	100
Arrival flow (veh/h)	1465	1498	541	562	1439	1407	435	458
Saturation flow (veh/h)	1801	1835	1830	1857	1862	1822	1824	1815
Transit bus penetration (%)	13	12	3	4	14	9	3	3
Passenger occupancy	20	20	20	20	20	20	20	20

green interval of the current phase determines the DPW growth closure point. In Figure 5(b), priority request responses at 20-second-TTOC, which means the actual green interval will be 20 s considering the green interval of fixed timing is 40 s, and phase two will show the maximum value because of the minimum remaining green among all phases.

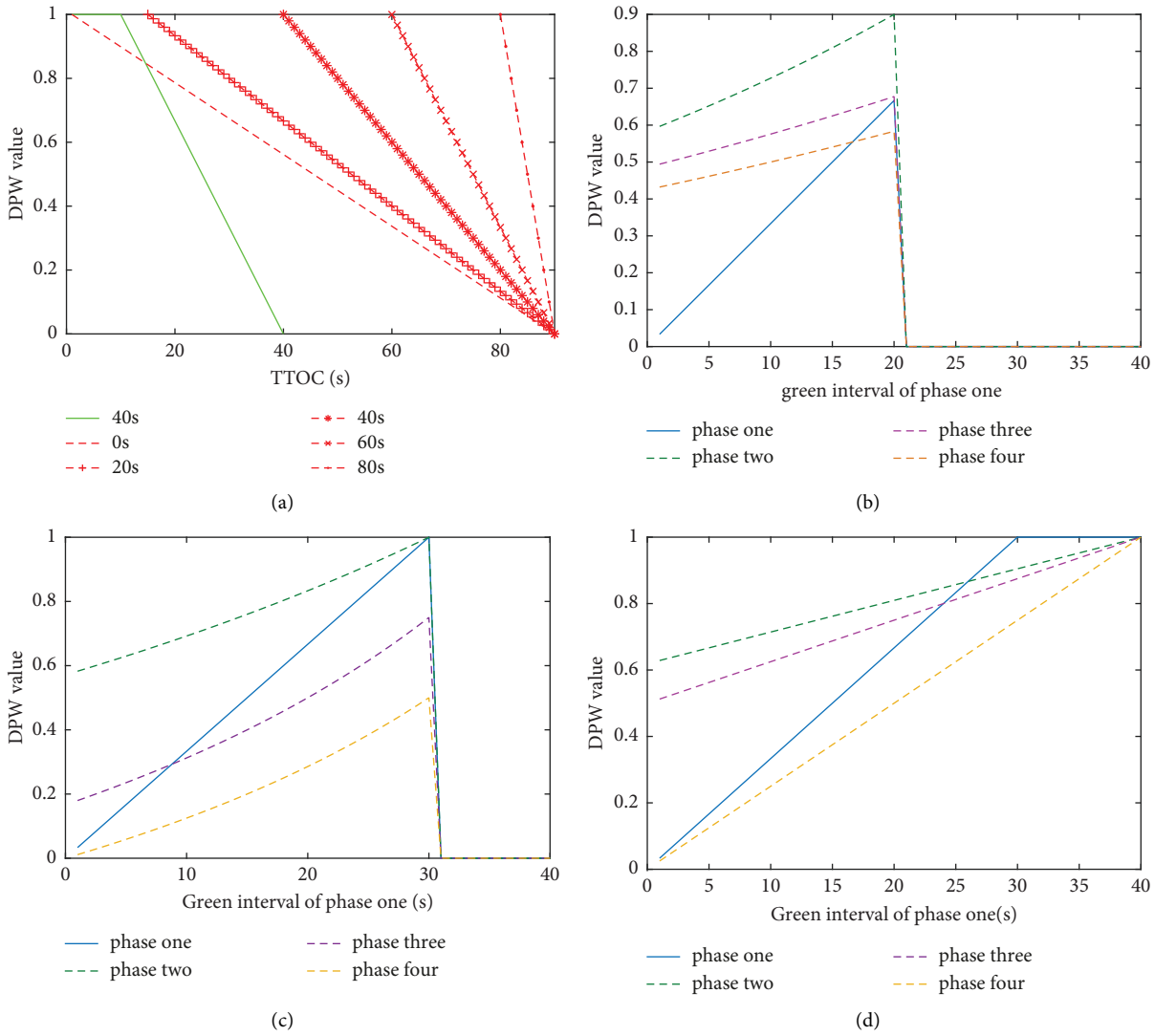

Figure 5: Single-vehicle DPW value with respect to TTOC. (a) Single-vehicle DPW value of phase one. (b) Red truncated at 20 s-TTOC. (c) Red truncated at 10 s-TTOC. (d) Red truncated at 0 s-TTOC of phase one.

In Figure 5(c), with time lapses, when TTOC is only 10 s (actual green interval equals 30), if priority request responses at that time, the single-vehicle DPW value of phase one reaches a peak and comes to equal with that of phase two. In Figure 5(d), when the TTOC of phase one decreases to zero (actual green interval equals 40), the single-vehicle DPW value of all phases grows to peak, that means if the TTOC of the current green phase is zero, all phases will have the equal chance to obtain green.

From the perspective of traffic demand measurement and traffic supply insurance, the increasing trend of DPW value of the conflict green phase reflects that vehicular waiting time strengthens the urgency of traffic demand, and the received priority request makes demand reach the maximum value to trigger phase switch for traffic supply achievement. After the current phase is switched to green, the decreasing trend of DPW value reflects the gradual release of demand. In the process of demand release, the demand of conflicting phases continues to accumulate to compete for green resources, the red interval of fixed timing determines the demand accumulation rate and competitive advantage. Once the phase switch and the traffic supply responses are completed, the DPW value of each phase will reset to the minimum value to realize the demand rebalance of all phases. Therefore, the changing trend of DPW value with TTOC is reasonable to describe the growth and decline process of traffic movement demand.

4.3. Comparative Simulation Experiment. While the numerical simulation results prove that the DPW model has the ability to measure the dynamic traffic demand of each movement, it does not consider any variability due to vehicle interactions and traffic flow fluctuation. As an open-source and highly portable, microscopic, and continuous multimodal traffic simulation package, simulation of urban mobility (SUMO) can assess the performance under more plausible conditions, which is used to evaluate the proposed

TSP logic under a connected vehicle environment in this paper. Included with SUMO is a wealth of supporting tools that automate core tasks for the creation, execution, and evaluation of traffic simulations, such as network import, route creation, and critical parameter configuration. Also, SUMO supplies a powerful traCI interface for online monitoring, interaction, and control. The evaluation is performed under the assumption that only transit buses are connected to traffic signal controllers and other social vehicles do not have V2X equipment. The data extracted are time, speed and position of the vehicle, number of vehicles passing the intersection, and volume from all four approaches. The traCI interface is also used to change the traffic signal timing plan during the simulation. All programs are coded in python.

The simulation network has been calibrated by manually editing intersection range, lane width, and stop line location, to match the real world shown in Figure 4. To reduce the saturation flow rate to a realistic range, the default settings of flow are redefined by omitting "speed" so that the calibrator will only affect flow by removing or insertion vehicles. After these adjustments, the saturation flow rate is reduced to 1823 veh/h on average. At least 10 simulation runs were performed for 12 hours with DPW-model-based signal control and without signal control (fixed timing). The minimum sample size requirement is checked to make the sure achievement of a sufficient number of simulations runs and statistical significance. The other parameter configuration in the simulation is the same as the ones in Table 1.

To evaluate the effectiveness of proposed priority actions, we use several disaggregated performance measures, minor traffic bus delay, minor traffic social vehicle delay, major traffic bus delay, major traffic social vehicle delay, average bus delay, and average social vehicle delay, expressed as seconds/vehicles. Furthermore, collected throughput flow rate and the number of queueing vehicle data are also used to assess the intersectional comprehensive performance benefits.

The rule-based TSP with handling conflicting requests (rule-based) method in literature [13] and TSP with connected vehicles accommodating conflicting requests (TSPCV-CR) method in literature [14] are selected for performance comparison analysis. For the Rule-based method, instead of taking any additional inputs for priority timing calculation except arrival time and occupancy, it takes the total person delay as the decision basis due to red truncation and green extension action on the respective. If there are buses on multiple approaches, an action executes to give priority to the corresponding approach that leads to the least total person delay. For the TSPCV-CR method, considering bus delay and social vehicle delay and importing occupancy parameters, it takes per person delay as the optimization objective to establish a BMILP model. For the reason why we choose two methods, it is because the rule-based method takes person delay as a phase switch decision variable without consideration of dynamic traffic demand measurement and secondary queue, which is the same in the delay of vehicle type and model solution complexity while is different at modelling process. As a typical programming algorithm, through performance comparison with TSPCV-CV, it can be helpful to prove that the DPW-based method is able to achieve near-optimal, or even optimal solutions. Besides that, highly similar research scenarios and research goals while different in optimization objectives are also in-negligible reasons.

4.3.1. Results and Discussion. With recordings of the number of queueing vehicles and the number of departure vehicles of each phase in twelve hours, we take ten minutes as a unit to calculate the cumulative number on average, then, we analyze the impacts on the capacity that DPW model-based signal control has, corresponding results are shown in Figures 6 and 7.

Figures 6(a)–6(h) show the queueing vehicle number variation of each phase under DPW model-based signal control enabled and disabled condition. It explains that the model has noticeable effects because of significant deduction on average queueing vehicle numbers at any timestamp of all phases. In addition, we can find out that the average queueing vehicle number fluctuation periods do not change, this is because though DPW model-based signal control supports phase switch anytime, to avoid causing possible control chaos, it postpones phase switch to move phase beginning time to the right, rather than makes frequent phase switch decision so as not to cut the cycle into more short phases.

This proves that our method is effective for green allocation without robustness sacrifice. From the green resource competition perspective, only if there are a greater number of queueing vehicles, would it have more desire to obtain green for that movement. What is more, it can be observed that the queueing vehicle number optimization is distinct for heavy traffic flow direction, there are huge drops at the tail of curves in Figures 6(a), 6(b), 6(e), and 6(f), and Figures 6(c), 6(d), 6(g), and 6(h) show slightly improved for slight traffic flow direction.

Figure 7 shows the departure vehicle number variation of each phase under DPW model-based signal control enabled and disabled conditions, it proves that the DPW model-based signal control does not result in inefficiency, inversely, contributing to capacity improvement. Cause performance benefits with control are obvious that vehicle departure number increases for almost all phases except for phase two and phase six, which reveal a faint decline at the end in Figures 7(b) and 7(f).

In terms of detail, it can be seen from Figures 7(e) and 7(h) that though DPW model-based method let green beginning time be put off, which causes vehicle departure numbers less than that of without control during some periods, e.g., 150–200 s and 400–450 s; however, throughput has been improved so that it almost reached the theoretical maximum. In Figures 6(c), 6(d), 6(g), and 6(h), the vehicle departure number experienced an enormous increase when the traffic light turns green, as a result of a larger number of the queueing vehicle at the end of red phase shown in the last figure.

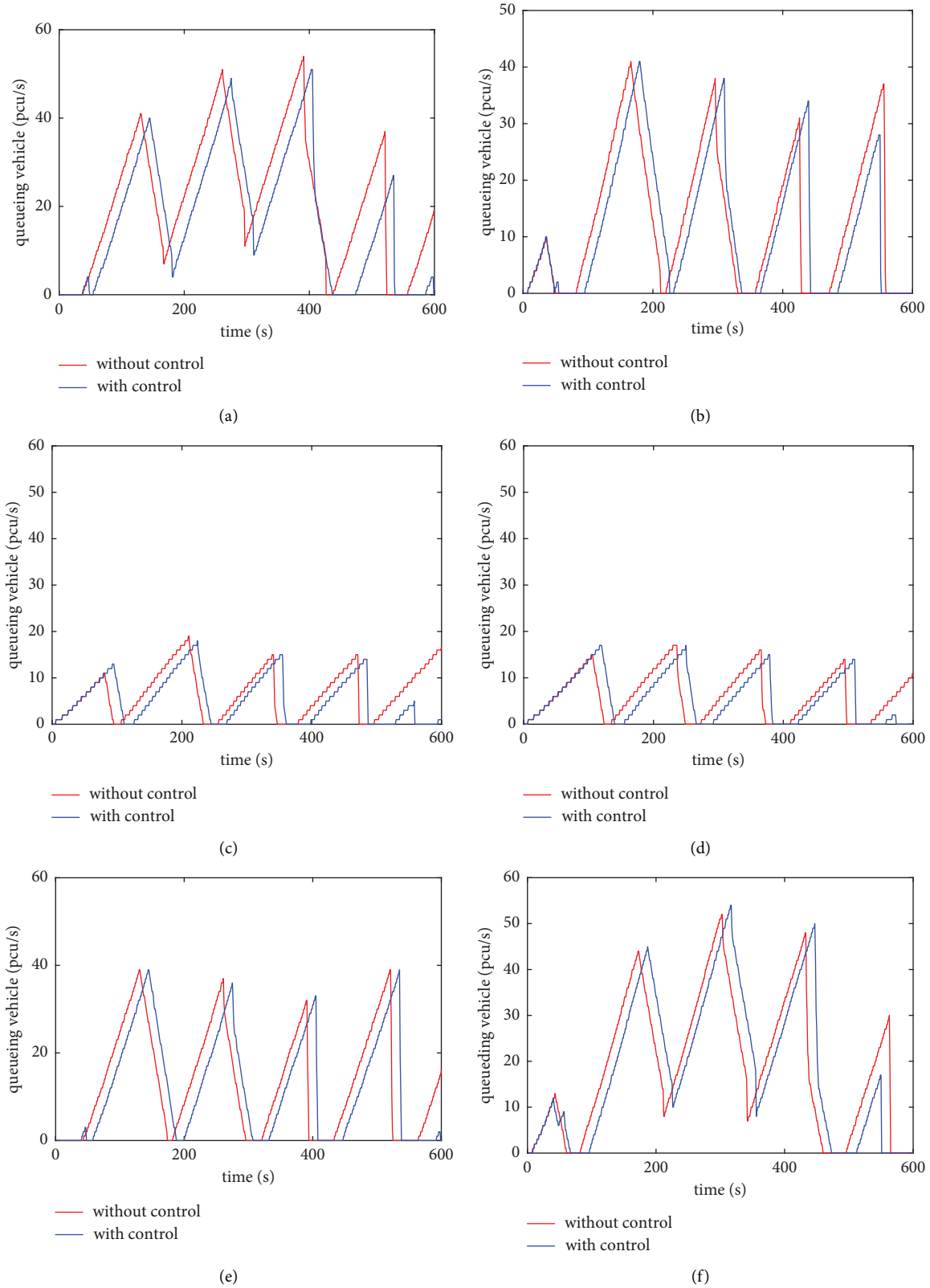

Figure 6: Continued.

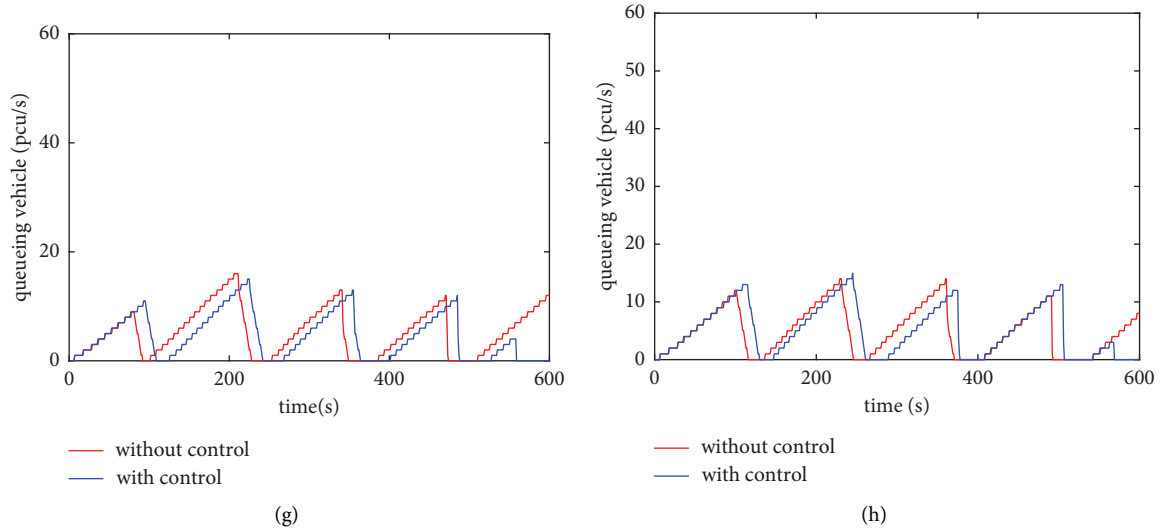

Figure 6: Comparison of queueing vehicle numbers with and without control. (a) Phase one. (b) Phase two. (c) Phase three. (d) Phase four. (e) Phase five. (f) Phase six. (g) Phase seven. (h) Phase eight.

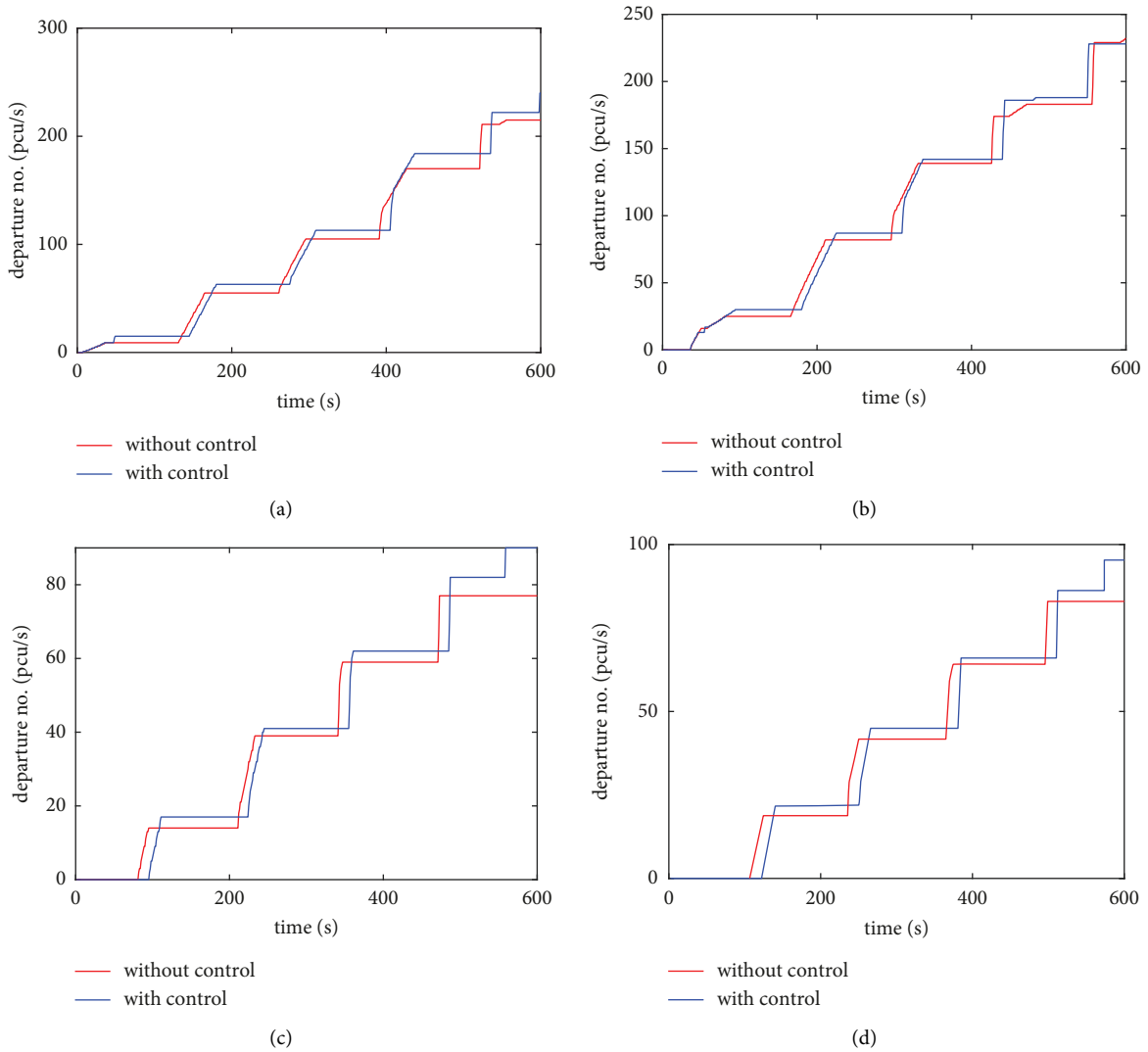

Figure 7: Continued.

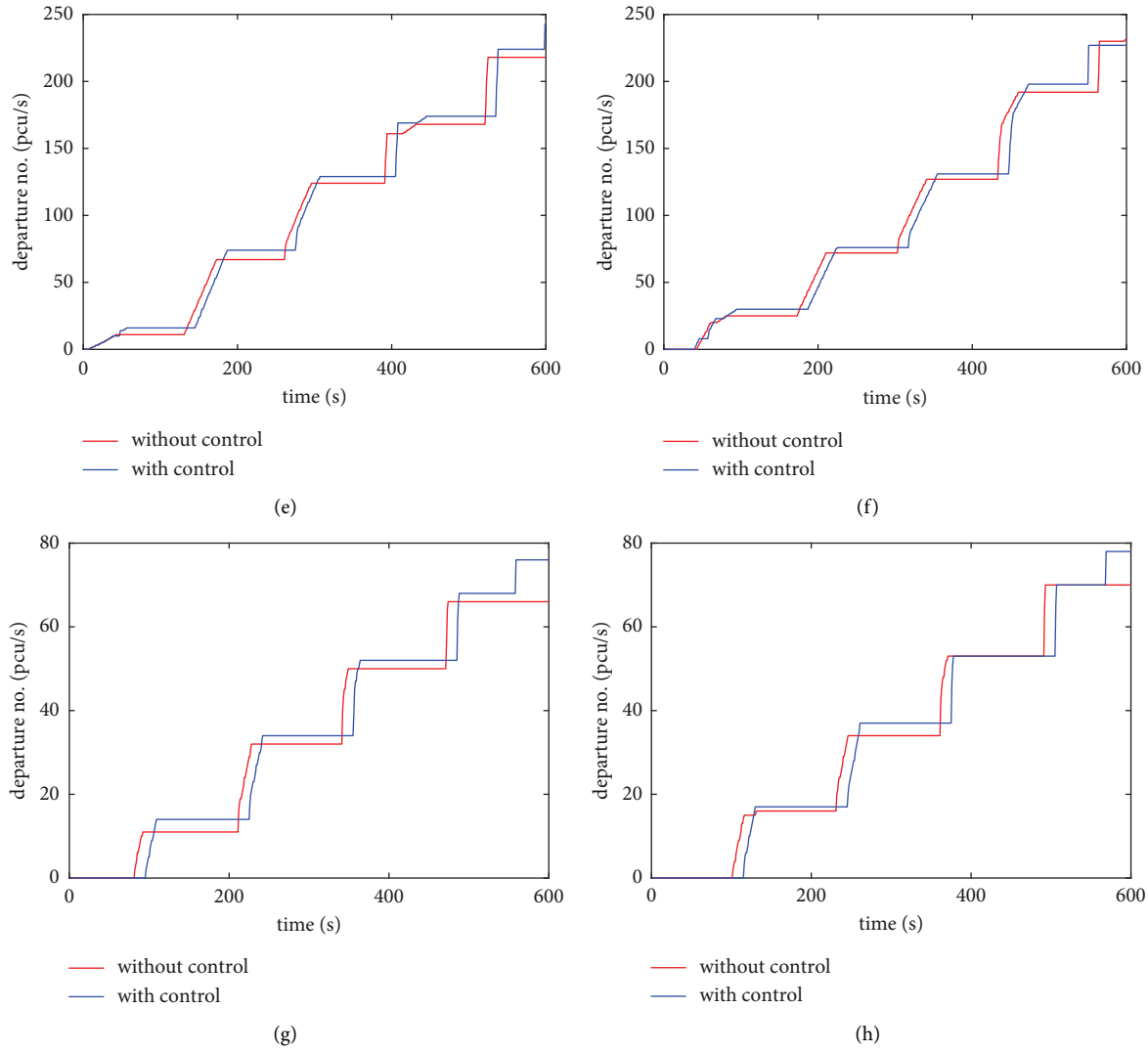

FIGURE 7: Comparison of vehicle departure numbers without and with control. (a) Phase one. (b) Phase two. (c) Phase three. (d) Phase four. (e) Phase five. (f) Phase six. (g) Phase seven. (h) Phase eight.

Even though the delay is neither the decision basis nor the optimization objective for DPW model-based method, to prove this method has superior performance in delay, we calculate the total delay based on the arrival and departure timestamp of each vehicle. Then, the average value is aggregated by vehicle type and traffic movement, which is shown in Figure 8.

Figure 8 compares the effects of fixed timing, Rule-based, TSPCV-CR, and DPW methods on delay performances. It can be seen from the figure that all methods greatly reduce bus delay and social vehicle delays compared to fixed timing control.

To be more specific, the DPW model-based method has the most excellent performance in average social vehicle delay. On the basis of fixed timing, the average bus delay optimized by rule-based, TSPCV-CR, and DPW methods is 21.4%, 34.76%, and 31.44%. Optimized average social vehicle delays show a downward trend in the ladder, which are 7.75%, 13.60%, and 22.11%. The rule-based method has the minimum optimization, especially indistinctively drop for the social vehicle delay. This is because, even though person delay of social vehicle is considered in the model, the conflicting requests resolution strategy is completely determined by delay duration, which makes buses with a high passenger occupancy have more competitive advantages for the green light, correspondingly, social vehicle priority is given away more. In addition, a lacking optimization solution and dynamic traffic demand measurement of traffic movement leads to the lowest degree of delay optimization. TSPCV-CR method takes per person delay as the optimization objective, which can achieve the bus delay optimization goal best of all. While for the DPW model-based method, the additional green extension is adopted to avoid secondary queuing of the bus in the queuing process so that

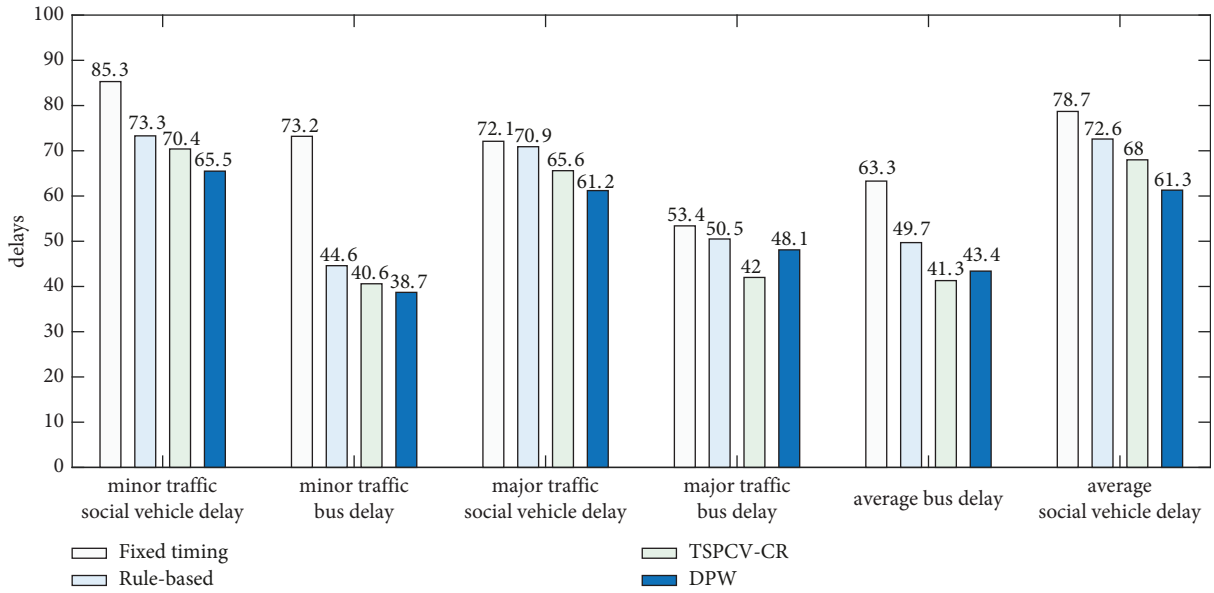

Figure 8: Delay comparison among fixed timing, TSPCV-CR, and DPW signal control method.

social vehicles in front of the queued bus can pass the intersection consequently, thus helping to reduce social vehicle delay more.

DPW model-based method has the most excellent delay performance for both minor and intersectional traffic movements. The average delay of these three methods for minor traffic movements is 117.9 (73.3 + 44.6), 111.0 (40.6 + 70.4), and 104.2 (38.7 + 65.5), for major traffic movements are 121.4 (70.9 + 50.5), 107.6 (42 + 65.6), and 109.3 (48.1 + 61.2), and for total delay is 122.3 (49.7 + 72.6), 109.3 (41.3 + 68), and 104.7 (43.4 + 61.3). The rule-based method has some degree of delay optimization for single movement and intersection overall; however, it is not nearly enough to be an ideal method compared to the other two methods because of disadvantages in different dimensions of delay. For the same reason explained in the last paragraph that lack of optimal solution and dynamic traffic demand modelling, delay-based decision mechanism may lose rationality, and unpredictability of accuracy for delay weakens the performance. Benefiting from the optimization solution, average bus delay achieves the best results for the TSPCV-CR method, it further improves the major traffic movement delay to be the smallest, but not enough to deduce intersectional delay overall by maximum. Compared to the TSPCV-CR method, the DPW model-based method reveals maximum delay drops even if more values for the average bus delay. This is because the traffic movement with a larger traffic volume and a higher proportion of transit buses, the more passengers will be, which makes the delay optimization space larger. DPW model-based method uses the aging timer to protect the right-of-way of the minor traffic movement to a certain extent, leading to greater improvements for delay of the minor traffic movement.

Therefore, considering the absolutely large proportion of social vehicles in practice, the DPW model-based method is more conducive to improve the overall traffic efficiency of the intersection and easing traffic congestion.

To give a more comprehensive evaluation and further validate the analysis conclusion in Figure 8, the number of queueing vehicles and throughput rate is calculated and aggregated by phase number to assess benefits performance on the basis of fixed timing. Figure 9 shows detailed benefits results of two indicators for the rule-based, TSPCV-CR, and DPW-based methods.

As shown in Figure 9, besides of slight decrease in queueing vehicle number of phase three by 0.09 pcu/s, the performance of other phases has been greatly optimized by the DPW model-based method. By comparison, the DPW model-based method has the largest benefits in queueing vehicle number and throughput flow rate among almost phases.

In Figure 9(a), the overall optimization range of queuing vehicle number of major traffic movements exceeds 1 pcu/s, which is about twice the overall optimization range of secondary traffic movements. The maximum increase in throughput rate reaches 3.34% for phase five, and the maximum reduction in queueing vehicle numbers is 1.69 for phase two. It is obvious that queueing vehicle number rarely exceeds 1 pcu/s for these phases, among which the indicator value is under 0.5 pcu/s indeed for the TSPCV-CR method. In stark contrast, the rule-based method has the minimum queue number benefits, instead of positive benefits for phase three and phase eight, negative benefits exist.

In Figure 9(b), the overall optimization range of the throughput rate of major traffic movements exceeds 2%, which is about twice the overall optimization range of secondary traffic movements for the DPW model-based method as well. The maximum increase in throughput rate reaches 3.34% for phase five. For the TSPCV-CR method, the throughput rate benefits of each phase are relatively

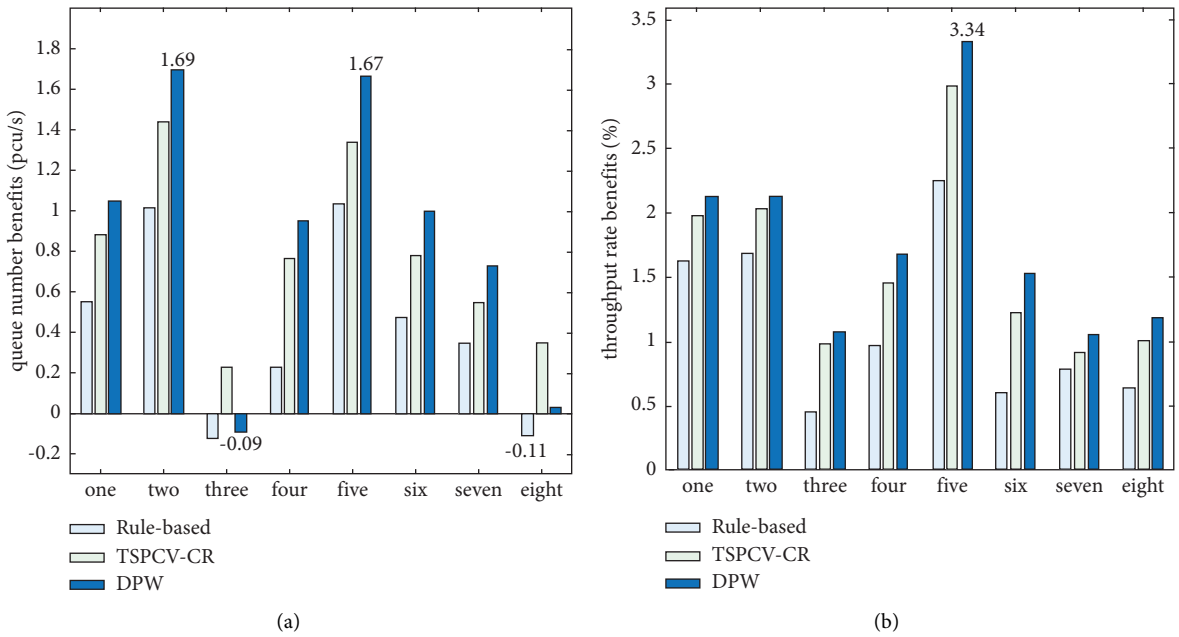

Figure 9: Performance benefits comparison between DPW-based and TSPCV-CR methods. (a) Queue number benefits. (b) Throughput rate benefits.

lower but considerably big. While for the rule-based method, throughput rate benefits show minimum positive value.

In general, the rule-based method shows weakness in both indicators for the single-phase dimension, even though there is a queue number benefits drawback for phase three and phase eight. Inferior performance benefits reveal for the TSPCV-CR method, however, it shows more equilibrated optimization than performance benefits of all phases experiencing positive growth, this explains that the TSPCV-CR method has a balanced optimization capacity for any traffic movements. It is worthy of notice for the DPW model-base method that throughput rate and queueing vehicle number still show the most significant improvement among all methods, even though there are a tiny amount of traffic capacity sacrifices for very few phases in exchange for better intersectional traffic service, this just proves the analysis conclusion in Figure 8 that DPW model-based method can improve the intersection efficiency better.

4.4. Field Test Data Analysis. To further verify the practical performance of the DPW-model-based signal control method, we deploy the algorithm software in MEC and carry out the field test. The experimental intersection is equipped with, a HIK TSC-500 signal controller of which green extension and red truncation functions are developed based on a software development kit, Huawei ATLAS-500 industrial control computer as MEC where Ascend A310 artificial intelligence chip is inside with the maximum hash rates of 22 TOPS, Huali's latest fifth generation RSU as the roadside device, which has cellular-V2X PC5 air interface. The comprehensive performance statistical table with daytime-twelve-hour field test data is listed in Table 3 to illustrate specific progress.

Table 3 gives a detailed description of the intersectional traffic capacity assessment. Compared with fixed timing control, the DPW model-based signal control algorithm has more positive effects on traffic capacity. Because the average queueing vehicle number and throughput flow rate in the "sum" column increase by 1.92 pcu/s and 6.68%, respectively. Both the average queueing vehicle number and throughput rate indicators show dramatic improvement, except for individual sacrifice in the average queueing number of phase three and throughput flow of phase four, which are 0.99 pcu/s and 0.11%.

Performance benefits show a similar trend that primary traffic movement profits almost more than secondary traffic movement. For primary traffic movement, phases one, two, five, and six, the average queueing vehicle number per second decreased by 2.94, 2.61, 3.34, 1.67, and throughput rates dramatically increased by 6.42%, 1.40%, 7.47%, and 12.29%. While for secondary movement, phases three, four, seven, and eight, there is less improvement except for the 9.98% throughput rate increase of phase seven, this is because phase seven has the lowest departure number for fixed timing that results in a huge optimization space.

By comparison, both field test and simulation results show that the proposed method has abilities to improve the traffic capacity of the intersection in typical cases and cause performance to show considerably positive benefits not only for almost all phases but also for intersectional capacity. This proves the effectiveness of conflicting request handling.

In addition, the performance benefits of the major traffic movement improve more for field tests. However, compared to the positive benefits in the throughput rate of phase four of simulation results, the sacrifice indicates that there are a few more negative impacts on some phases of minor traffic movements in practical, which emphasizes the analysis

Table 3: Comprehensive performance parameter statistic.

	Phase no.	One	Two	Three	Four	Five	Six	Seven	Eight	Sum/ave
Fixed timing	Average queueing vehicle no.(pcu/s)	9.28	7.88	2.87	13.49	7.81	8.81	7.76	7.98	8.24
	Departure vehicle no.(pcu)	20216	21205	8945	9805	20475	19222	6563	7423	113854
	Arrival vehicle no.(pcu)	23904	23940	10106	10102	23941	23946	8474	8471	132884
	Throughput rate (%)	84.57	88.58	88.51	87.95	85.52	87.27	87.45	87.63	87.19
DPW	Average queueing vehicle no.(pcu/s)	6.34	5.27	3.86	10.05	4.47	7.14	7.36	6.05	6.32
	Departure vehicle no.(pcu)	19371	19139	7939	7757	19789	21190	7203	6542	109430
	Arrival vehicle no.(pcu)	21288	21271	8832	8831	21280	21284	7393	7392	117571
	Throughput rate (%)	90.99	89.98	89.89	87.84	92.99	99.56	97.43	88.50	93.87
Benefits	Average queueing vehicle no.(pcu/s)	2.94	2.61	−0.99	3.44	3.34	1.67	0.4	1.93	1.92
	Throughput rate (%)	6.42	1.40	1.38	−0.11	7.47	12.29	9.98	0.87	6.68

concluded that the DPW model-based method scarifies a tiny amount of traffic capacity for minor traffic movement in exchange for better intersectional traffic service.

What is more, the overall optimization ranges of queuing vehicle numbers and throughput rate of major traffic movements are about twice the overall optimization range of secondary traffic movements for simulation results. For field test results, the overall optimization ranges of major traffic movements almost exceed 2 pcu/s and 6% respectively, both the average and maximum value of field test results transcend that of simulation results.

As for reasons why there are additional performance sacrifices for minor traffic movement, arrival flow from major traffic movement in the field test exceeds 100 vehicles for one hour than that of in the simulation experiment, so the traffic condition comes to slight oversaturation. To avoid secondary queueing, the algorithm has to make this choice to guarantee intersectional capacity maximized so as not to be unable to pass the intersection for vehicles' arrival in minor traffic movement.

In summary, even though there are additional performance losses for the field test in a critical minor traffic movement, trading off comparative advantages in major traffic movements, this loss can be completely absorbed. As the same evaluation standard is used for two types of experiments, the difference in results between simulation and the field test just goes to indicate that this method has practical application potential.

5. Conclusion

This paper proposes a signal control approach to coordinate multi-directional conflicting priority requests at a signalized intersection. The proposed approach takes advantage of connected transit buses' motion and signal timing data as two unique input parameters. Typically, theb TTOC of the current phase, transit bus locations, and the current phase are used to measure the total prioritized weight of each phase. This paper includes three parts: an aggregated weighted DPW model for vehicle arrival during the effective green of the current phase and the conflict phase, a multidirectional conflicting phase resolution control method, and a comparative analysis of performance evaluation with both a simulation experiment and a field test.

Experimental results indicate that the final manifestation pattern shows similarity to cycle length translation to the right for some seconds by the proposed DPW model-based signal control method. It not only has the ability to tackle multidirectional conflicting priority request problems but also improve the traffic efficiency of the intersection. In the under-saturated circumstance environment, via the completely real-time computation of the aggregated weighted DPW value of each phase and adequately flexible control for phase switching, the proposed method can decrease the average queueing vehicle number of almost all phases and increase the throughput rate of the intersection, where the benefits of the two indicators are 1.92 pcu/s and 6.68% generally.

Compared to the algorithm with delay as the decision basis and objective, even though more delay exists for arrival vehicles in major traffic movements and throughput rate regression occurs in some phases of minor traffic movements, the DPW-based method has the biggest improvements in traffic capacities, not only for major traffic movements but also for the overall intersection. In the current traffic flow environment where social vehicles account for an absolute proportion, even though the person delay-based programming algorithm shows better performance promotion for bus delay with 41.3 s in average, this method shows more preference for social vehicles (61.3 s delay) while declining bus delay with an appreciable quantity with 43.4 s in average.

DPW-based method has the largest benefits not only in queueing vehicle numbers but also in throughput flow rate among almost all phases. For the DPW-based method, the overall optimization ranges of queuing vehicle number and throughput rate for major traffic movements exceed 1 pcu/s and 2%, respectively. For the TSPCV-CR method, queue number benefits rarely exceed 1 pcu/s for these phases, among which the indicator value is indeed under 0.5 pcu/s, and the throughput rates of each phase are obviously lower. While for the rule-based method, the overall optimization degree is the lowest among these three methods, there are negative benefits for some phases. So, considering much more substantial improvements in intersectional traffic capacity, the DPW-based method proposed in this paper has more practical application value in the present.

There are some limitations to this study. In terms of the unified dynamic priority weight function, the single-vehicle DPW value is only related to their own location besides TTOC without consideration of the other vehicular factor, thus there is some space for model optimization.

In the future, further work on the DPW model will focus on introducing a location argument and exploring improving throughput under higher traffic flow and density conditions because vehicle queueing and queue clearance will probably be heterogeneous and seriously influenced under the oversaturated circumstance. Additional works will be done for performance observation in large density scenarios and to find out the optimum throughput equilibrium point at the intersection of disequilibrium traffic supply and demand.

Data Availability

The data used to support the findings of this study are available from the author upon reasonable request.

Conflicts of Interest

The authors declare that they have no conflicts of interest.

Authors' Contributions

SH, HH, and TZQ carried out the study conception and design; SH and HZ collected the data; SH and SS performed the analysis and interpretation of results; SH, HZ, and TZQ prepared the draft manuscript. All authors reviewed the results and approved the final version of the manuscript.

Acknowledgments

This research was jointly supported by Major Science and Technology Project of Zhejiang Province, Bilateral Industry Joint R&D Program Project "Research and Application of Intelligent Highway Technology Based on Vehicle-Road Cooperation" (Project no. 2021C04007) and Key Research and Develop Projects in Hainan Province (Project no. ZDYF2021GXJS015).

References

[1] W. Qiao, W. Ding, and H. Jia, *Reliability Oriented Transit Signal Priority System*, TRB, 2018.

[2] J. Li, Y. Liu, H. Yang, and B. Chen, "Bus priority signal control considering delays of passengers and pedestrians of adjacent intersections," *Journal of Advanced Transportation*, vol. 2020, Article ID 3935795, 12 pages, 2020.

[3] Z. Liang, Y. Xiao, and Y. P. Flötteröd, "An overlapping phase approach to optimize bus signal priority control under two-way signal coordination on urban arterials," *Journal of Advanced Transportation*, vol. 2021, Article ID 6624130, 13 pages, 2021.

[4] E. Christofa, K. Ampountolas, and A. Skabardonis, "Arterial traffic signal optimization: a person-based approach," *Transportation Research Part C: Emerging Technologies*, vol. 66, pp. 27–47, 2016.

[5] L. Feng and W. Jian, "Active transit signal priority considering overlapping phase in artery progression," in *Proceedings of the International Conference on Advanced Computer Control IEEE*, Shenyang, China, March 2010.

[6] S. Yagar and B. Han, "A procedure for real-time signal control that considers transit interference and priority," *Transportation Research Part B: Methodological*, vol. 28, no. 4, pp. 315–331, 1994.

[7] Q. He, K. L. Head, and J. Ding, "Heuristic algorithm for priority traffic signal control," *Transportation Research Record Journal of the Transportation Research Board*, vol. 2259, pp. 1–7, 2011.

[8] S. Xianmin, Y. Mili, L. Di, and M. Lin, "Optimization method for transit signal priority considering multirequest under connected vehicle environment," *Journal of Advanced Transportation*, vol. 2018, Article ID 7498594, 10 pages, 2018.

[9] W. Ma, Y. Liu, and X. Yang, "A dynamic programming approach for optimal signal priority control upon multiple high-frequency bus requests," *Journal of Intelligent Transportation Systems*, vol. 17, no. 4, pp. 282–293, 2013.

[10] X. Zeng, Y. Zhang, K. N. Balke, and K. Yin, "A real-time transit signal priority control model considering stochastic bus arrival time," *IEEE Transactions on Intelligent Transportation Systems*, vol. 15, no. 4, pp. 1657–1666, 2014.

[11] Y. Lin, X. Yang, G. L. Chang, and N. Zou, "Transit priority strategies for multiple routes under headway-based operations," *Transportation Research Record: Journal of the Transportation Research Board*, vol. 2356, no. 1, pp. 34–43, 2013.

[12] J. Lee and A. Shalaby, "Rule-based transit signal priority control method using a real-time transit travel time prediction model," *Canadian Journal of Civil Engineering*, vol. 40, no. 1, pp. 68–75, 2013.

[13] B. T. Thodi, B. R. Chilukuri, and L. Vanajakshi, "An analytical approach to real-time bus signal priority system for isolated intersections," *Journal of Intelligent Transportation Systems*, vol. 26, no. 2, pp. 145–167, 2022.

[14] J. Hu, B. B. Park, and Y. J. Lee, "Transit signal priority accommodating conflicting requests under connected vehicles technology," *Transportation Research Part C: Emerging Technologies*, vol. 69, pp. 173–192, 2016.

[15] H. Liu, K. Teng, L. Rai, and J. Xing, "Transit signal priority controlling method considering non-transit traffic benefits and coordinated phase states for multi-rings timing plan at isolated intersections," *IEEE Transactions on Intelligent Transportation Systems*, vol. 22, no. 2, pp. 913–936, 2021.

[16] C. Colombaroni, G. Fusco, and N. Isaenko, "A simulation-optimization method for signal synchronization with bus priority and driver speed advisory to connected vehicles," *Transportation Research Procedia*, vol. 45, pp. 890–897, 2020.

[17] Y. Jiang, Z. Liu, Z. Hu, and H. Zhang, "A priority-based conflict resolution strategy for airport surface traffic considering suboptimal alternative paths," *IEEE Access*, vol. 9, pp. 606–617, 2021.

[18] Y. Feng, K. L. Head, S. Khoshmagham, and M. Zamanipour, "A real-time adaptive signal control in a connected vehicle environment," *Transportation Research Part C: Emerging Technologies*, vol. 55, pp. 460–473, 2015.

[19] H. Chai, H. M. Zhang, D. Ghosal, and C.-N. Chuah, "Dynamic traffic routing in a network with adaptive signal control," *Transportation Research Part C: Emerging Technologies*, vol. 85, pp. 64–85, 2017.

[20] S. Kim, M. Park, and K. S. Chon, "Bus signal priority strategies for multi-directional bus routes," *KSCE Journal of Civil Engineering*, vol. 16, no. 5, pp. 855–861, 2012.

[21] M. Zamanipour, K. L. Head, Y. Feng, and S. Khoshmagham, "Efficient priority control model for multimodal traffic signals," *Transportation Research Record: Journal of the Transportation Research Board*, vol. 2557, no. 1, pp. 86–99, 2016.

[22] Q. He, K. L. Head, and J. Ding, "Multi-modal traffic signal control with priority, signal actuation and coordination," *Transportation Research Part C: Emerging Technologies*, vol. 46, pp. 65–82, 2014.

[23] Y. Ren, J. Zhao, and X. Zhou, "Optimal design of scheduling for bus rapid transit by combining with passive signal priority control," *International Journal of Sustainable Transportation*, vol. 15, no. 5, pp. 407–418, 2020.

[24] K. Wu, M. Lu, and S. I. Guler, "Modeling and optimizing bus transit priority along an arterial: a moving bottleneck approach," *Transportation Research Part C: Emerging Technologies*, vol. 121, no. 5, Article ID 102873, 2020.

[25] Q. He, K. L. Head, and J. Ding, "PAMSCOD: p," *Transportation Research Part C: Emerging Technologies*, vol. 20, no. 1, pp. 164–184, 2012.

[26] M. Xu, K. An, Z. Ye, Y. Wang, J. Feng, and J. Zhao, "A bi-level model to resolve conflicting transit priority requests at urban arterials," *IEEE Transactions on Intelligent Transportation Systems*, vol. 20, pp. 1353–1364, 2019.

[27] K. Wu and S. I. Guler, "Estimating the impacts of transit signal priority on intersection operations: a moving bottleneck approach," *Transportation Research Part C: Emerging Technologies*, vol. 105, pp. 346–358, 2019.

[28] W. Zhou, Y. Bai, J. Li, and Y. Zhou, "Integrated optimization of tram schedule and signal priority at intersections to minimize person delay," *Journal of Advanced Transportation*, vol. 2019, pp. 1–18, 2019.

[29] F. Dion and B. Hellinga, "A rule-based real-time traffic responsive signal control system with transit priority: application to an isolated intersection," *Transportation Research Part B: Methodological*, vol. 36, no. 4, pp. 325–343, 2002.